In another clinical trial of a synthetic peptide vaccine, IC41 containing the 7 relevant HCV-specific Th cell and CTL epitopes and the adjuvant poly-L-arginine were used. It has been reported that IC41 can induce HCV-specific responses in both Th1 cells and CTLs in patients not responding to or relapsing from IFN therapy [72, 73]. Although this vaccination was tolerated and induced serious adverse events, HCV RNA reduction was rarely observed in the study [73]. In the phase II trial of pegylated interferon plus ribavirin therapy in combination with this vaccine, an enhanced HCV-specific T-cell response was observed in 73% of patients, and the responses could be detected more frequently in patients with sustained virologic response than in those showing relapse [74].

A recent Phase I placebo-controlled study has revealed that a prototype vaccine, which consists of HCV core protein and the adjuvant ISCOMATRIX, induces cytokine production by T-cells, but CTL responses were detected in a few healthy individuals [75]. A tableted therapeutic bivalent vaccine, which consists of heat-inactivated HCV antigens derived from HBV- and HCV-infected donors, has been applied in the treatment of chronic hepatitis C patients. Oral administration of this vaccine showed no adverse effects, and the elevated liver enzyme levels observed before the study were reduced in all patients at the end of the study.

A therapeutic DNA vaccine developed using the mixture of plasmid expressing HCV structural antigens and a recombinant HCV core protein, namely, CIGB-230, has also been used to treat chronic hepatitis C patients who did not respond to previous IFN therapy in a Phase I study [76]. This vaccination induced specific T-cell responses in 73% of the participants. Interestingly, 40% of the vaccinated patients showed reduction in liver fibrosis.

5. Conclusions and Future Directions

Since HCV was first identified, many investigations have been performed to resolve and prevent HCV infection. It has been demonstrated that HCV-specific CTLs are implicated in not only viral eradication but also the immunopathogenesis of hepatitis C. Development of IFN-based therapy in combination with ribavirin and protease/polymerase inhibitor has improved the sustained viral response rate of patients. However, there are still many nonresponders who suffer from chronic hepatitis C, cirrhosis, and hepatocellular carcinoma. Moreover, the HCV infection mechanism in many patients is still unknown. For these patients, a novel immune therapy and vaccination should be urgently established. For this purpose, we have to continue further investigation of immune responses in HCV infection.

References

[1] Q.-L. Choo, G. Kuo, A. J. Weiner, L. R. Overby, D. W. Bradley, and M. Houghton, "Isolation of a cDNA clone derived from a blood-borne non-A, non-B viral hepatitis genome," *Science*, vol. 244, no. 4902, pp. 359–362, 1989.

[2] K. L. Yap, G. L. Ada, and I. F. C. McKenzie, "Transfer of specific cytotoxic T lymphocytes protects mice inoculated with influenza virus," *Nature*, vol. 273, no. 5659, pp. 238–239, 1978.

[3] R. M. Zinkernagel, E. Haenseler, T. Leist, A. Cerny, H. Hengartner, and A. Althage, "T cell-mediated hepatitis in mice infected with lymphocytic choriomeningitis virus. Liver cell destruction by H-2 class I-restricted virus-specific cytotoxic T cells as a physiological correlate of the 51Cr-release assay?" *Journal of Experimental Medicine*, vol. 164, no. 4, pp. 1075–1092, 1986.

[4] C. E. Samuel, "Antiviral actions of interferons," *Clinical Microbiology Reviews*, vol. 14, no. 4, pp. 778–809, 2001.

[5] Y.-J. Liu, H. Kanzler, V. Soumelis, and M. Gilliet, "Dendritic cell lineage, plasticity and cross-regulation," *Nature Immunology*, vol. 2, no. 7, pp. 585–589, 2001.

[6] H. Watarai, E. Sekine, S. Inoue, R. Nakagawa, T. Kaisho, and M. Taniguchi, "PDC-TREM, a plasmacytoid dendritic cell-specific receptor, is responsible for augmented production of type I interferon," *Proceedings of the National Academy of Sciences of the United States of America*, vol. 105, no. 8, pp. 2993–2998, 2008.

[7] A. Ahmad and F. Alvarez, "Role of NK and NKT cells in the immunopathogenesis of HCV-induced hepatitis," *Journal of Leukocyte Biology*, vol. 76, no. 4, pp. 743–759, 2004.

[8] J. Banchereau and R. M. Steinman, "Dendritic cells and the control of immunity," *Nature*, vol. 392, no. 6673, pp. 245–252, 1998.

[9] D. Kägi, F. Vignaux, B. Ledermann, et al., "Fas and perforin pathways as major mechanisms of T cell-mediated cytotoxicity," *Science*, vol. 265, no. 5171, pp. 528–530, 1994.

[10] H. Kojima, N. Shinohara, S. Hanaoka, et al., "Two distinct pathways of specific killing revealed by perforin mutant cytotoxic T lymphocytes," *Immunity*, vol. 1, no. 5, pp. 357–364, 1994.

[11] K. Ando, K. Hiroishi, T. Kaneko, et al., "Perforin, Fas/Fas ligand, and TNF-α pathways as specific and bystander killing mechanisms of hepatitis C virus-specific human CTL," *Journal of Immunology*, vol. 158, no. 11, pp. 5283–5291, 1997.

[12] K. Ando, T. Moriyama, L. G. Guidotti, et al., "Mechanisms of class I restricted immunopathology. A transgenic mouse model of fulminant hepatitis," *Journal of Experimental Medicine*, vol. 178, no. 5, pp. 1541–1554, 1993.

[13] H. Doi, K. Hiroishi, T. Shimazaki, et al., "Magnitude of $CD8^+$ T-cell responses against hepatitis C virus and severity of hepatitis do not necessarily determine outcomes in acute hepatitis C virus infection," *Hepatology Research*, vol. 39, no. 3, pp. 256–265, 2009.

[14] G. M. Lauer, E. Barnes, M. Lucas, et al., "High resolution analysis of cellular immune responses in resolved and persistent hepatitis C virus infection," *Gastroenterology*, vol. 127, no. 3, pp. 924–936, 2004.

[15] D. Yerly, D. Heckerman, T. M. Allen, et al., "Increased cytotoxic T-lymphocyte epitope variant cross-recognition and functional avidity are associated with hepatitis C virus clearance," *Journal of Virology*, vol. 82, no. 6, pp. 3147–3153, 2008.

[16] K. Hiroishi, H. Kita, M. Kojima, et al., "Cytotoxic T lymphocyte response and viral load in hepatitis C virus infection," *Hepatology*, vol. 25, no. 3, pp. 705–712, 1997.

[17] S. Zeuzem, "Hepatitis C virus: kinetics and quasispecies evolution during anti-viral therapy," *Forum*, vol. 10, no. 1, pp. 32–42, 2000.

[18] S. Guglietta, A. R. Garbuglia, L. Salichos, et al., "Impact of viral selected mutations on T cell mediated immunity in chronically evolving and self limiting acute HCV infection," *Virology*, vol. 386, no. 2, pp. 398–406, 2009.

[19] A. L. Hughes, M. A. K. Hughes, and R. Friedman, "Variable intensity of purifying selection on cytotoxic T-lymphocyte epitopes in hepatitis C virus," *Virus Research*, vol. 123, no. 2, pp. 147–153, 2007.

[20] A. Maki, M. Matsuda, M. Asakawa, H. Kono, H. Fujii, and Y. Matsumoto, "Decreased CD3 ζ molecules of T lymphocytes from patients with hepatocellular carcinoma associated with hepatitis C virus," *Hepatology Research*, vol. 27, no. 4, pp. 272–278, 2003.

[21] G. Missale, E. Cariani, and C. Ferrari, "Role of viral and host factors in HCV persistence: which lesson for therapeutic and preventive strategies?" *Digestive and Liver Disease*, vol. 36, no. 11, pp. 703–711, 2004.

[22] V. Francavilla, D. Accapezzato, M. De Salvo, et al., "Subversion of effector $CD8^+$ T cell differentiation in acute hepatitis C virus infection: exploring the immunological mechanisms," *European Journal of Immunology*, vol. 34, no. 2, pp. 427–437, 2004.

[23] S. Urbani, B. Amadei, D. Tola, et al., "PD-1 expression in acute hepatitis C virus (HCV) infection is associated with HCV-specific CD8 exhaustion," *Journal of Virology*, vol. 80, no. 22, pp. 11398–11403, 2006.

[24] L. Golden-Mason, B. Palmer, J. Klarquist, J. A. Mengshol, N. Castelblanco, and H. R. Rosen, "Upregulation of PD-1 expression on circulating and intrahepatic hepatitis C virus-specific $CD8^+$ T cells associated with reversible immune dysfunction," *Journal of Virology*, vol. 81, no. 17, pp. 9249–9258, 2007.

[25] L. Golden-Mason, J. Klarquist, A. S. Wahed, and H. R. Rosen, "Cutting edge: programmed death-1 expression is increased on immunocytes in chronic hepatitis C virus and predicts failure of response to antiviral therapy: race-dependent differences," *Journal of Immunology*, vol. 180, no. 6, pp. 3637–3641, 2008.

[26] N. Nakamoto, H. Cho, A. Shaked, et al., "Synergistic reversal of intrahepatic HCV-specific CD8 T cell exhaustion by combined PD-1/CTLA-4 blockade," *PLoS Pathogens*, vol. 5, no. 2, Article ID e1000313, 2009.

[27] M. Kriegs, T. Bürckstümmer, K. Himmelsbach, et al., "The hepatitis C virus non-structural NS5A protein impairs both the innate and adaptive hepatic immune response in vivo," *Journal of Biological Chemistry*, vol. 284, no. 41, pp. 28343–28351, 2009.

[28] Z. Q. Yao, D. T. Nguyen, A. I. Hiotellis, and Y. S. Hahn, "Hepatitis C virus core protein inhibits human T lymphocyte responses by a complement-dependent regulatory pathway," *Journal of Immunology*, vol. 167, no. 9, pp. 5264–5272, 2001.

[29] D. J. Kittlesen, K. A. Chianese-Bullock, Z. Q. Yao, T. J. Braciale, and Y. S. Hahn, "Interaction between complement receptor gC1qR and hepatitis C virus core protein inhibits T-lymphocyte proliferation," *Journal of Clinical Investigation*, vol. 106, no. 10, pp. 1239–1249, 2000.

[30] Z. Q. Yao, A. Eisen-Vandervelde, S. Ray, and Y. S. Hahn, "HCV core/gC1qR interaction arrests T cell cycle progression through stabilization of the cell cycle inhibitor p27Kip1," *Virology*, vol. 314, no. 1, pp. 271–282, 2003.

[31] K. V. Konan, T. H. Giddings Jr., M. Ikeda, K. Li, S. M. Lemon, and K. Kirkegaard, "Nonstructural protein precursor NS4A/B from hepatitis C virus alters function and ultrastructure of host secretory apparatus," *Journal of Virology*, vol. 77, no. 14, pp. 7843–7855, 2003.

[32] P. Sarobe, J. J. Lasarte, A. Zabaleta, et al., "Hepatitis C virus structural proteins impair dendritic cell maturation and inhibit in vivo induction of cellular immune responses," *Journal of Virology*, vol. 77, no. 20, pp. 10862–10871, 2003.

[33] G. Szabo and A. Dolganiuc, "Subversion of plasmacytoid and myeloid dendritic cell functions in chronic HCV infection," *Immunobiology*, vol. 210, no. 2–4, pp. 237–247, 2005.

[34] P.-Y. Lozach, H. Lortat-Jacob, A. de Lacroix de Lavalette, et al., "DC-SIGN and L-SIGN are high affinity binding receptors for hepatitis C virus glycoprotein E2," *Journal of Biological Chemistry*, vol. 278, no. 22, pp. 20358–20366, 2003.

[35] S. Pöhlmann, J. Zhang, F. Baribaud, et al., "Hepatitis C virus glycoproteins interact with DC-SIGN and DC-SIGNR," *Journal of Virology*, vol. 77, no. 7, pp. 4070–4080, 2003.

[36] C. Aloman, S. Gehring, P. Wintermeyer, N. Kuzushita, and J. R. Wands, "Chronic ethanol consumption impairs cellular immune responses against HCV NS5 protein due to dendritic cell dysfunction," *Gastroenterology*, vol. 132, no. 2, pp. 698–708, 2007.

[37] T. Boettler, H. C. Spangenberg, C. Neumann-Haefelin, et al., "T cells with a $CD4^+CD25^+$ regulatory phenotype suppress in vitro proliferation of virus-specific $CD8^+$ T cells during chronic hepatitis C virus infection," *Journal of Virology*, vol. 79, no. 12, pp. 7860–7867, 2005.

[38] D. Accapezzato, V. Francavilla, M. Paroli, et al., "Hepatic expansion of a virus-specific regulatory $CD8^+$ T cell population in chronic hepatitis C virus infection," *Journal of Clinical Investigation*, vol. 113, no. 7, pp. 963–972, 2004.

[39] M. Sakaki, K. Hiroishi, T. Baba, et al., "Intrahepatic status of regulatory T cells in autoimmune liver diseases and chronic viral hepatitis," *Hepatology Research*, vol. 38, no. 4, pp. 354–361, 2008.

[40] A. J. MacDonald, M. Duffy, M. T. Brady, et al., "CD4 T helper type 1 and regulatory T cells induced against the same epitopes on the core protein in hepatitis C virus-infected persons," *Journal of Infectious Diseases*, vol. 185, no. 6, pp. 720–727, 2002.

[41] F. Belardelli, "Role of interferons and other cytokines in the regulation of the immune response," *APMIS*, vol. 103, no. 3, pp. 161–179, 1995.

[42] S.-H. Fang, L.-H. Hwang, D.-S. Chen, and B.-L. Chiang, "Ribavirin enhancement of hepatitis C virus core antigen-specific type 1 T helper cell response correlates with the increased IL-12 level," *Journal of Hepatology*, vol. 33, no. 5, pp. 791–798, 2000.

[43] D. F. Tough, P. Borrow, and J. Sprent, "Induction of bystander T cell proliferation by viruses and type I interferon in vivo," *Science*, vol. 272, no. 5270, pp. 1947–1950, 1996.

[44] K. Hiroishi, T. Tüting, and M. T. Lotze, "IFN-α-expressing tumor cells enhance generation and promote survival of tumor-specific CTLs," *Journal of Immunology*, vol. 164, no. 2, pp. 567–572, 2000.

[45] S. Gehring, S. H. Gregory, N. Kuzushita, and J. R. Wands, "Type 1 interferon augments DNA-based vaccination against hepatitis C virus core protein," *Journal of Medical Virology*, vol. 75, no. 2, pp. 249–257, 2005.

[46] C. B. Willberg, S. M. Ward, R. F. Clayton, et al., "Protection of hepatocytes from cytotoxic T cell mediated killing by interferon-alpha," *PLoS One*, vol. 2, no. 8, article e791, 2007.

[47] A. J. Freeman, G. Marinos, R. A. Ffrench, and A. R. Lloyd, "Intrahepatic and peripheral blood virus-specific cytotoxic T lymphocyte activity is associated with a response to combination IFN-α and ribavirin treatment among patients with chronic hepatitis C virus infection," *Journal of Viral Hepatitis*, vol. 12, no. 2, pp. 125–129, 2005.

[48] H. Kita, T. Moriyama, T. Kaneko, et al., "HLA B44-restricted cytotoxic T lymphocytes recognizing an epitope on hepatitis C virus nucleocapsid protein," *Hepatology*, vol. 18, no. 5, pp. 1039–1044, 1993.

[49] H. Kita, K. Hiroishi, T. Moriyama, et al., "A minimal and optimal cytotoxic T cell epitope within hepatitis C virus nucleoprotein," *Journal of General Virology*, vol. 76, no. 12, pp. 3189–3193, 1995.

[50] T. Kaneko, I. Nakamura, H. Kita, K. Hiroishi, T. Moriyama, and M. Imawari, "Three new cytotoxic T cell epitopes identified within the hepatitis C virus nucleoprotein," *Journal of General Virology*, vol. 77, no. 6, pp. 1305–1309, 1996.

[51] T. Hakamada, K. Funatsuki, H. Morita, et al., "Identification of novel hepatitis C virus-specific cytotoxic T lymphocyte epitopes by ELISpot assay using peptides with human leukocyte antigen-A*2402-binding motifs," *Journal of General Virology*, vol. 85, no. 6, pp. 1521–1531, 2004.

[52] K. Ito, K. Shiraki, K. Funatsuki, et al., "Identification of novel hepatitis C virus-specific cytotoxic T lymphocyte epiotpe in NS3 region," *Hepatology Research*, vol. 36, no. 4, pp. 294–300, 2006.

[53] T. Mashiba, K. Udaka, Y. Hirachi, et al., "Identification of CTL epitopes in hepatitis C virus by a genome-wide computational scanning and a rational design of peptide vaccine," *Immunogenetics*, vol. 59, no. 3, pp. 197–209, 2007.

[54] Y. Takao, A. Yamada, S. Yutani, et al., "Identification of new immunogenic peptides in conserved regions of hepatitis C virus (HCV) 1b with the potentiality to generate cytotoxic T lymphocytes in HCV1b$^+$HLA-A24$^+$ patients," *Hepatology Research*, vol. 37, no. 3, pp. 186–195, 2007.

[55] S. Matsueda, A. Yamada, Y. Takao, et al., "A new epitope peptide derived from hepatitis C virus 1b possessing the capacity to induce cytotoxic T-lymphocytes in HCV1b-infected patients with HLA-A11, -A31, and -A33," *Cancer Immunology, Immunotherapy*, vol. 56, no. 9, pp. 1359–1366, 2007.

[56] D. Yerly, D. Heckerman, T. Allen, et al., "Design, expression, and processing of epitomized hepatitis C virus-encoded CTL epitopes," *Journal of Immunology*, vol. 181, no. 9, pp. 6361–6370, 2008.

[57] T. Kaneko, T. Moriyama, K. Udaka, et al., "Impaired induction of cytotoxic T lymphocytes by antagonism of a weak agonist borne by a variant hepatitis C virus epitope," *European Journal of Immunology*, vol. 27, no. 7, pp. 1782–1787, 1997.

[58] S. Gehring, S. H. Gregory, P. Wintermeyer, M. San Martin, C. Aloman, and J. R. Wands, "Generation and characterization of an immunogenic dendritic cell population," *Journal of Immunological Methods*, vol. 332, no. 1-2, pp. 18–30, 2008.

[59] S. Gehring, S. H. Gregory, P. Wintermeyer, C. Aloman, and J. R. Wands, "Generation of immune responses against hepatitis C virus by dendritic cells containing NS5 protein-coated microparticles," *Clinical and Vaccine Immunology*, vol. 16, no. 2, pp. 163–171, 2009.

[60] H. Yu, H. Huang, J. Xiang, L. A. Babiuk, and S. van Drunen Littel-van den Hurk, "Dendritic cells pulsed with hepatitis C virus NS3 protein induce immune responses and protection from infection with recombinant vaccinia virus expressing NS3," *Journal of General Virology*, vol. 87, no. 1, pp. 1–10, 2006.

[61] P. Li, Q. Wan, Y. Feng, et al., "Engineering of *N*-glycosylation of hepatitis C virus envelope protein E2 enhances T cell responses for DNA immunization," *Vaccine*, vol. 25, no. 8, pp. 1544–1551, 2007.

[62] M. Liu, H. Chen, F. Luo, et al., "Deletion of N-glycosylation sites of hepatitis C virus envelope protein E1 enhances specific cellular and humoral immune responses," *Vaccine*, vol. 25, no. 36, pp. 6572–6580, 2007.

[63] P. Martin, B. Simon, Y.-C. Lone, et al., "A vector-based minigene vaccine approach results in strong induction of T-cell responses specific of hepatitis C virus," *Vaccine*, vol. 26, no. 20, pp. 2471–2481, 2008.

[64] D. Thammanichanond, S. Moneer, P. Yotnda, et al., "Fiber-modified recombinant adenoviral constructs encoding hepatitis C virus proteins induce potent HCV-specific T cell response," *Clinical Immunology*, vol. 128, no. 3, pp. 329–339, 2008.

[65] A. A. Haller, G. M. Lauer, T. H. King, et al., "Whole recombinant yeast-based immunotherapy induces potent T cell responses targeting HCV NS3 and Core proteins," *Vaccine*, vol. 25, no. 8, pp. 1452–1463, 2007.

[66] Q. Qiu, R. Y.-H. Wang, X. Jiao, et al., "Induction of multi-specific Th-1 type immune response against HCV in mice by protein immunization using CpG and Montanide ISA 720 as adjuvants," *Vaccine*, vol. 26, no. 43, pp. 5527–5534, 2008.

[67] C. Hartoonian, M. Ebtekar, H. Soleimanjahi, et al., "Effect of immunological adjuvants: GM-CSF (granulocyte-monocyte colony stimulating factor) and IL-23 (interleukin-23) on immune responses generated against hepatitis C virus core DNA vaccine," *Cytokine*, vol. 46, no. 1, pp. 43–50, 2009.

[68] G. Liao, Y. Wang, J. Chang, et al., "Hepatitis B virus precore protein augments genetic immunizations of the truncated hepatitis C virus core in BALB/c mice," *Hepatology*, vol. 47, no. 1, pp. 25–34, 2008.

[69] A. Memarnejadian and F. Roohvand, "Fusion of HBsAg and prime/boosting augment Th1 and CTL responses to HCV polytope DNA vaccine," *Cellular Immunology*, vol. 261, no. 2, pp. 93–98, 2010.

[70] Y. Niu, N. Komatsu, Y. Komohara, et al., "A peptide derived from hepatitis C virus (HCV) core protein inducing cellular-responses in patients with HCV with various HLA class IA alleles," *Journal of Medical Virology*, vol. 81, no. 7, pp. 1232–1240, 2009.

[71] S. Yutani, N. Komatsu, S. Shichijo, et al., "Phase I clinical study of a peptide vaccination for hepatitis C virus-infected patients with different human leukocyte antigen-class I-A alleles," *Cancer Science*, vol. 100, no. 10, pp. 1935–1942, 2009.

[72] V. Schlaphoff, C. S. Klade, B. Jilma, et al., "Functional and phenotypic characterization of peptide-vaccine-induced HCV-specific CD8$^+$ T cells in healthy individuals and chronic hepatitis C patients," *Vaccine*, vol. 25, no. 37-38, pp. 6793–6806, 2007.

[73] C. S. Klade, H. Wedemeyer, T. Berg, et al., "Therapeutic vaccination of chronic hepatitis C nonresponder patients with the peptide vaccine IC41," *Gastroenterology*, vol. 134, no. 5, pp. 1385–1395.e1, 2008.

[74] H. Wedemeyer, E. Schuller, V. Schlaphoff, et al., "Therapeutic vaccine IC41 as late add-on to standard treatment in patients with chronic hepatitis C," *Vaccine*, vol. 27, no. 37, pp. 5142–5151, 2009.

[75] D. Drane, E. Maraskovsky, R. Gibson, et al., "Priming of CD4$^+$ and CD8$^+$ T cell responses using a HCV core ISCOMATRIX^{TM} vaccine: a phase I study in healthy volunteers," *Human Vaccines*, vol. 5, no. 3, pp. 151–157, 2009.

[76] L. Alvarez-Lajonchere, N. H. Shoukry, B. Grá, et al., "Immunogenicity of CIGB-230, a therapeutic DNA vaccine preparation, in HCV-chronically infected individuals in a Phase I clinical trial," *Journal of Viral Hepatitis*, vol. 16, no. 3, pp. 156–167, 2009.

J Gastroenterol (2010) 45:451–458
DOI 10.1007/s00535-009-0155-2

ORIGINAL ARTICLE—LIVER, PANCREAS, AND BILIARY TRACT

Strong CD8$^+$ T-cell responses against tumor-associated antigens prolong the recurrence-free interval after tumor treatment in patients with hepatocellular carcinoma

Kazumasa Hiroishi · Junichi Eguchi · Toshiyuki Baba · Tomoe Shimazaki · Shigeaki Ishii · Ayako Hiraide · Masashi Sakaki · Hiroyoshi Doi · Shojiro Uozumi · Risa Omori · Takuya Matsumura · Tatsuro Yanagawa · Takayoshi Ito · Michio Imawari

Received: 10 August 2009 / Accepted: 19 October 2009 / Published online: 20 November 2009

Abstract
Aim We investigated whether tumor-specific CD8$^+$ T-cell responses affect tumor-free survival as well as the relationship between CD8$^+$ T-cell responses against tumor-associated antigens (TAAs) and the clinical course after tumor treatment in patients with hepatocellular carcinoma (HCC).
Methods Twenty patients with HCC that were treated by radiofrequency ablation or trans-catheter chemo-embolization (TACE) and in whom HCC was undetectable by ultrasonography, CT, and/or MRI 1 month after treatment were enrolled in the study. Before and after treatment for HCC, analyses of TAA (glypican-3, NY-ESO-1, and MAGE-1)-specific CD8$^+$ T-cell responses were evaluated with an interferon-γ enzyme-linked immunospot (ELISpot) assay using peripheral CD8$^+$ T-cells, monocytes, and 104 types of 20-mer synthetic peptide overlapping by 10 residues and spanning the entirety of the 3 TAAs.
Results Sixteen out of 20 patients (80%) showed a positive response ($\geq$10 TAA-specific cells/10^5 CD8$^+$ T-cells) before or after treatment. When we performed univariate analysis of prognostic factors for the tumor-free period in the 20 patients, platelet count, prothrombin time, and the number of TAA-specific CD8$^+$ T-cells after treatment were significant factors ($P = 0.027$, 0.030, and 0.004, respectively). In multivariate analysis, the magnitude of the TAA-specific CD8$^+$ T-cell response ($\geq$40 TAA-specific cells/10^5 CD8$^+$ T-cells) was the only significant prognostic factor for a prolonged tumor-free interval (hazard ratio 0.342, $P = 0.022$).
Conclusions Our results suggest that strong TAA-specific CD8$^+$ T-cell responses suppress the recurrence of HCC. Immunotherapy to induce TAA-specific cytotoxic T lymphocytes by means such as the use of peptide vaccines should be considered for clinical application in patients with HCC after local therapy.

Keywords Hepatocellular carcinoma · CD8$^+$ T-cell response · Cytotoxic T lymphocyte · ELISpot assay · Immunotherapy

K. Hiroishi · J. Eguchi · T. Baba · T. Shimazaki · S. Ishii · A. Hiraide · M. Sakaki · H. Doi · S. Uozumi · R. Omori · T. Matsumura · T. Yanagawa · T. Ito · M. Imawari (✉)
Division of Gastroenterology, Department of Medicine, Showa University School of Medicine, 1-5-8 Hatanodai, Shinagawa-ku, Tokyo 142-8666, Japan
e-mail: imawari@med.showa-u.ac.jp

Introduction

There are about 500,000 new patients with hepatocellular carcinoma (HCC) per year worldwide. Although vaccination against hepatitis B virus (HBV) and interferon (IFN)-based therapy against hepatitis C virus (HCV) will presumably reduce the number of HCC patients in the future, the incidence of HCC is still increasing in Asia and Africa because of the previous prevalence of infection with the virus. Progress in treatments for HCC has improved the prognosis of patients with HCC. However, HCC is usually associated with cirrhosis and often recurs even after complete treatment of the tumors in the remaining part of the cirrhotic liver. Thus, there is a strong need for the development of a new intervention therapy that suppresses the occurrence or recurrence of HCC effectively and that has fewer side effects. Immunotherapy may be such a treatment and may be applicable to the clinical treatment of HCC. In fact, some clinical trials have been performed [1–3].

Cytotoxic T lymphocytes (CTLs) are thought to be potent effector cells against cancers. CTLs recognize specific antigens, and the induction of CTLs specific for tumor-associated antigen (TAA) is an attractive procedure

for tumor therapy. The MAGE-1 gene was first identified as encoding a tumor-specific antigen on MZ-2-MEL cells, a melanoma cell line, in 1991 [4]. MAGE-1 gene and protein can be detected in many cancer tissues, and three articles reported the expression of MAGE-1 in HCC as 30, 68, or 78%, respectively, in a Japanese population [5–7]. In gastrointestinal tumors, immunotherapy using both dendritic cells and MAGE peptides has been performed for patients with primary malignant melanoma of the esophagus, and this therapy was able to induce peptide-specific immune responses [8].

NY-ESO-1 antigen, a member of the cancer-testis antigen family, was initially identified by a serological analysis of recombinant cDNA expression cloning in an esophageal cancer patient [9]. NY-ESO-1 mRNA was detected in 24–37% of HCCs by reverse transcription-polymerase chain reaction [10, 11].

Glypican-3 (GPC3) consists of 580 amino acids and is a heparan sulfate proteoglycan with a potential role in the control of cell division. GPC3 mRNA was detected in 74.8% of HCC tissues, but only in 3.2% of normal liver tissues [12], and GPC3 protein was detected in 72% of HCCs, but not in normal tissue using GPC-specific antibody [13]. The GPC3 protein can also be detected in sera of 40–53% of patients with HCC [14, 15].

These three antigens are thought to be attractive targets for cancer immunotherapy because they are expressed only in tumor tissues and testis, but not in normal tissues other than testis. On the basis of previous reports, it is assumed that most HCCs would express at least one of the three TAAs. Therefore, monitoring immune responses against these TAAs might help in the development of HCC immunotherapy, such as TAA-based vaccination. In this study, we investigated how the magnitude of $CD8^+$ T-cell responses against these TAAs determined by an IFN-γ enzyme-linked immunospot (ELISpot) assay is related to other clinical data and the tumor-free interval in patients with HCC, in order to explore the clinical application of such a TAA-based immunotherapy.

Methods

Patients

Twenty patients who were diagnosed with HCC at Showa University Hospital between 2006 and 2008 were enrolled in the study. They met the following study criteria: (1) pathologically confirmed as having HCC or a lesion with characteristic imaging features of HCC based on ultrasonography, CT, and/or MRI; (2) liver function classed as Child-Pugh A or B; (3) no extrahepatic metastasis or vascular invasion; (4) no previous or simultaneous cancers other than HCC; and (5) an indication for treatment such as radiofrequency ablation (RFA) or trans-catheter chemo-embolization (TACE). RFA was performed by well-trained hepatologists using usual methods according to previous reports [16]. A 16-gauge cooled-tip ablation electrode (Covidien, Boulder, CO) was used in the procedure. TACE was performed by well-experienced hepatologists and radiologists. A microcatheter was inserted from the femoral artery to the artery feeding the HCC superselectively after conventional hepatic angiography, and then a segmental or subsegmental TACE procedure was performed using gelatin, lipiodol, and either epirubicin hydrochloride or cisplatin. All patients were followed every 1–3 months by ultrasonography, CT, and/or MRI to examine the appearance of new lesions in the liver or other organs. The recurrence-free interval was defined as the period from the month of HCC treatment to the month when a recurrent and/or metastatic HCC was first detected after treatment. Clinical data (platelet count, prothrombin time, serum AST, ALT, albumin, total bilirubin level, and AFP level) were collected 1–7 days before HCC treatment. Chronic hepatitis C was diagnosed on the basis of detectable HCV RNA in serum using the Amplicor assay (Roche Diagnostics, Tokyo, Japan). Informed consent was obtained from each patient included in this study. The study protocol conformed to the ethical guidelines of the 1975 Declaration of Helsinki as reflected in a priori approval by the Ethical Committee of Showa University.

Synthetic peptides of TAA

Twenty-mer peptides overlapping by 10 residues and spanning the entire MAGE-1, NY-ESO-1, and GPC3 proteins were synthesized based on the amino acid sequences reported previously as PepSets™ and purchased from Mimotopes (Clayton South, Victoria, Australia). These peptides were >80% pure. A total of 30 MAGE-1, 17 NY-ESO-1, and 57 GPC3 peptides were synthesized, as shown in Table 1. A total of 10–11 TTA peptides were pooled in a mixture (total 10 mixtures) at a concentration of 10 μg/ml each.

Preparation of $CD8^+$ T cells and monocytes from patients with HCC

PBMCs were isolated from heparinized peripheral blood by gradient centrifugation using Ficoll-Paque (Pharmacia-LKB Biotechnology, Uppsala, Sweden). As reported previously, peripheral $CD8^+$ T-cells and monocytes were separated from PBMCs using CD8 microbeads (MACS system; Miltenyi Biotec, Bergisch Gladbach, Germany) and a Monocyte Isolation Kit II (Miltenyi Biotec), respectively [17]. These cells were isolated using an autoMACS™ Pro Separator (Miltenyi Biotec). The purity of the cells was >95% on flow cytometry (data not shown).

Table 1 Synthetic peptides and peptide mixtures used in this study

Tumor-associated antigen	Peptide	Amino acid sequence
Glypican-3	GL1	1–20
	GL2	11–30
	GL3	21–40
	⋮	⋮
	GL57	561–580
MAGE-1	MG-1	1–20
	⋮	⋮
	MG-30	290–309
NY-ESO-1	NY-1	1–20
	⋮	⋮
	NY-17	161–180

Mix 1	Mix 2	Mix 3	Mix 4	Mix 5	Mix 6	Mix 7	Mix 8	Mix 9	Mix 10
GL1	GL2	GL3	GL4	GL5	GL6	GL7	GL8	GL9	GL10
GL11	GL12	GL13	GL14	GL15	GL16	GL17	GL18	GL19	GL20
GL21	GL22	GL23	GL24	GL25	GL26	GL27	GL28	GL29	GL30
GL31	GL32	GL33	GL34	GL35	GL36	GL37	GL38	GL39	GL40
GL41	GL42	GL43	GL44	GL45	GL46	GL47	GL48	GL49	GL50
GL51	GL52	GL53	GL54	GL55	GL56	GL57	MG-1	MG-2	MG-3
MG-4	MG-5	MG-6	MG-7	MG-8	MG-9	MG-10	MG-11	MG-12	MG-13
MG-14	MG-15	MG-16	MG-17	MG-18	MG-19	MG-20	MG-21	MG-22	MG-23
MG-24	MG-25	MG-26	MG-27	MG-28	MG-29	MG-30	NY-1	NY-2	NY-3
NY-4	NY-5	NY-6	NY-7	NY-8	NY-9	NY-10	NY-11	NY-12	NY-13
NY-14	NY-15	NY-16	NY-17	–	–	–	–	–	–

IFN-γ ELISpot assay

The ELISpot assay was performed using an IFN-γ ELISpot assay kit (Mabtech AB, Stockholm, Sweden) as previously described [17]. Briefly, a 96-well microtiter plate with a nitrocellulose membrane bottom (Millititer; Millipore, Bedford, MA) was coated with 100 μl anti-IFN-γ monoclonal antibody at a concentration of 15 μg/ml in phosphate-buffered saline (PBS) overnight at 4°C. Unbound antibody was removed by washing 6 times in Hanks' balanced saline solution. After blocking with AIM-V medium (Invitrogen Japan, Tokyo, Japan) containing 10% fetal bovine serum, 1×10^5 $CD8^+$ T-cells, 1×10^4 autologous monocytes, and a TAA peptide mixture at 10 μg/ml of each peptide were placed and incubated in duplicate in 100 μl AIM-V medium at 37°C in a humid atmosphere with 5% CO_2. After incubation for 18 h, the cells were removed by washing the plate 8 times with PBS. Next, 100 μl of biotin-conjugated monoclonal antibody was added to each well, and the plates were incubated further for 2 h at room temperature. Wells were washed 5 times with PBS and incubated with 100 μl streptavidin–alkaline phosphatase for 2 h. Unbound antibodies were removed by washing 6 times with PBS. Then, 100 μl of alkaline phosphatase substrate (Bio-Rad Laboratories, Richmond, CA) was added to each well and incubated until dark spots emerged. Color development was stopped by washing 3 times with water, and the plates were allowed to dry. Using an ELISpot reader (KS ELISPOT compact; Carl Zeiss, Oberkochen, Germany), the number of spot-forming cells (SFCs) per well was counted. Numbers of TAA-specific SFCs for each peptide mixture were calculated by subtracting the mean number of SFCs of 2 control wells (without stimulus) from the mean number of SFCs of 2 wells stimulated by TAA antigens. An SFC number was calculated for each patient as the sum of SFCs in each peptide mixture. ELISpot assays were performed before and 3–7 days after treatment. When TAA-specific $CD8^+$ T-cell responses were analyzed in 10 normal subjects, we were unable to detect any responses against TAA peptides in the ELISpot assay (data not shown).

Statistical analyses

The relationship between the number of TAA-specific $CD8^+$ T-cells and the recurrence-free period was analyzed

using a parametric survival model. The log-rank test was used to compare recurrence-free data for 2 groups. The effects of multiple explanatory variables on recurrence-free interval were analyzed using a Cox proportional hazards model. Statistical analyses were performed using the statistical software JMP version 5 (SAS Institute Inc., Cary, NC). Differences were considered as significant when the P value was less than 0.05.

Results

TAA-specific CD8$^+$ T-cells were detected by ELISpot assay before and after HCC treatment in most HCC patients

The characteristics of the 20 patients enrolled in this study are shown in Table 2. The 20 patients had no HCC detected by ultrasonography, enhanced CT, and/or MRI 1 month after treatment for HCC. In those patients with HCCs who had up to 3 HCCs and in whom the diameter of each lesion was 3 cm or less, the treatment was usually RFA; the remaining patients were treated by TACE. However, in a few patients (patients 2 and 5) in whom the diameter of each lesion was less than 3 cm, the physician in charge of the patient selected TACE because they could not deny the existence of more lesions that were undetectable by conventional enhanced CT. The clinical courses of the patients were followed for 3–29 months after therapy for HCC. The ELISpot assay was performed to detect CD8$^+$ T-cell responses to TAAs before and 3–7 days after treatment. The data are shown in Table 3 as SFCs (total count of TAA-specific CD8$^+$ T-cells/1 $\times$ 10^5 CD8$^+$ T-cells). Sixteen out of 20 patients (80%) showed a positive response (10 or more SFCs) for TAA peptides either before and/or after treatment. The numbers of SFCs (mean $\pm$ SD) before and after therapy were 33.8 $\pm$ 51.4 (0–161, median 16.5) and 32.9 $\pm$ 34.7 (0–130, median 23.0), respectively. Of the 20 patients, 5 (25%) and 7 (35%) showed a high TAA-specific immune response (40 or more SFCs) before and after treatment, respectively.

When we analyzed the TAA peptides recognized by CD8$^+$ T-cells, we occasionally observed that different peptide mixtures were identified as positive before and after HCC treatment (data not shown).

Change in TAA-specific CD8$^+$ T-cell response induced by HCC treatment does not correlate with recurrence-free period

The number of SFCs increased in 11 of 20 (55%) patients after treatment. In these patients, TAA-specific CTLs might have been induced by the treatment. There were no significant differences between the increase in TAA-specific CD8$^+$ T-cell response induced by the treatment and either therapeutic procedure, laboratory data, or background of the patients (data not shown). The increase in TAA-specific CTLs after treatment did not predict a better prognosis of HCC.

Table 2 Characteristics of HCC patients before HCC treatment

	$n = 20$	Median
Age (years)[a]	68.8 $\pm$ 9.4	73.0
Gender		
M	11	
F	9	
AST (IU/l)[a]	70 $\pm$ 49	52
ALT (IU/l)[a]	63 $\pm$ 43	54
PLT ($\times 10^4/\mu$l)[a]	9.8 $\pm$ 5.3	8.5
PT (%)[a]	81 $\pm$ 11	78
Alb (g/dl)[a]	3.5 $\pm$ 0.4	3.4
T-Bil (mg/dl)[a]	0.9 $\pm$ 0.4	0.9
AFP (ng/ml)[a]	86 $\pm$ 157	16
Virus		
HCV	17	
NBNC	3	
Child-Pugh class		
A	12	
B	8	
HCC size (mm)[a]	23 $\pm$ 8	23
No. HCCs		
1	9	
2	4	
3	7	
>3	0	
Treatment		
RFA	13	
TACE	5	
RFA + TACE	2	

NBNC Negative for neither HBV nor HCV infection, *RFA* radiofrequency ablation, *TACE* trans-catheter chemo-embolization

[a] Results are shown as mean $\pm$ SD

Platelet count, prothrombin time, and the magnitude of TAA-specific immune response after treatment correlate with the recurrence-free period by univariate analysis

When we analyzed the relationship between TAA-specific SFCs detected by the ELISpot assay or other clinical variates and the HCC-free interval using a parametric survival model, we found that platelet count, prothrombin time, and the TAA-specific CD8$^+$ T-cell response after treatment significantly correlated with the HCC-free interval

Table 3 Results of IFN-γ ELISpot assay in patients in whom HCCs were not detected after therapy

Patient no.	SFC before treatment (/10^5 $CD8^+$ T-cells)	SFC after treatment (/10^5 $CD8^+$ T-cells)	Recurrence-free interval (month)
1	0	0	5
2	15	31	10
3	12	15	5
4	159	130	26
5	58	4	12
6	5	99	29[a]
7	15	17	7
8	20	41	7
9	135	9	12
10	1	6	3
11	8	9	6
12	10	57	15
13	34	42	13[a]
14	6	4	12[a]
15	23	8	9
16	59	37	12
17	12	29	23
18	161	72	24
19	18	4	15
20	25	44	23[a]

SFC Spot-forming cells

[a] These patients had no recurrence detected by ultrasonography, enhanced CT, and/or MRI after treatment

($P = 0.005$, 0.007, and 0.001, respectively). When univariate analysis of prognostic factors for the HCC-free interval was performed, only platelet count ($P = 0.027$; Fig. 1a), prothrombin time ($P = 0.030$; Fig. 1b), and the number of SFCs after treatment ($P = 0.004$; Fig. 1c) were found to be significant. Child-Pugh class A tended to prolong the HCC-free interval, although this was not significant ($P = 0.066$). The other factors, including the number of SFCs before treatment ($P = 0.407$), ALT level ($P = 0.644$), albumin level ($P = 0.488$), total bilirubin level ($P = 0.340$), HCC size ($P = 0.756$), HCC number ($P = 0.486$), and the procedure used for HCC treatment (RFA or TACE, $P = 0.481$), did not affect HCC-free survival, as confirmed by the log-rank test.

Multivariate analysis shows that the magnitude of TAA-specific $CD8^+$ T-cell responses correlates with the HCC-free interval after treatment in patients who have no detectable HCC after therapy

In a further analysis of the 20 patients with HCC who were treated by RFA or TACE and in whom no HCC was detectable 1 month after treatment, we performed multivariate analysis using a Cox proportional hazards model. On multivariate analysis, only the magnitude of TAA-specific $CD8^+$ T-cell responses (≥40 TAA-specific cells/10^5 $CD8^+$ T-cells) was the only significant prognostic factor for a prolonged tumor-free period after treatment

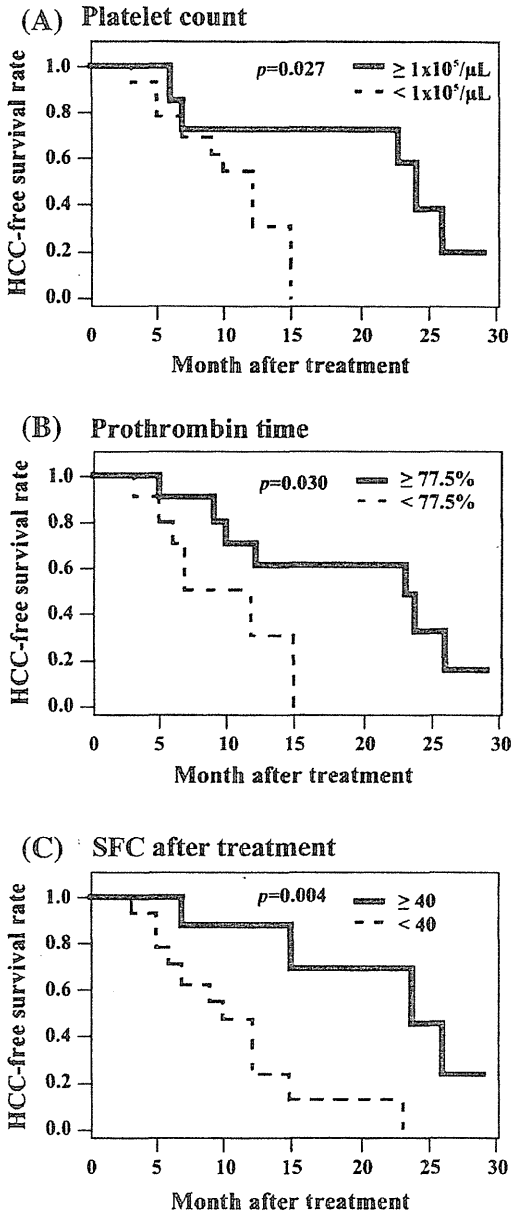

Fig. 1 Kaplan–Meier curves of HCC-free survival rate. In univariate analysis, platelet count, prothrombin time, and the tumor-associated antigen-specific $CD8^+$ T-cell response were found to be prognostic factors for the HCC-free period after treatment. Kaplan–Meier curves representing the relationship between month after treatment (HCC-free interval) and HCC-free survival rate were grouped by **a** platelet count, **b** prothrombin time, and **c** spot-forming cells (*SFCs*) specific for tumor-associated antigens after treatment

Table 4 Multivariate analyses of prognostic factors for tumor-free interval

Variable	Hazard ratio	95% Confidence limit	*P* value
Platelet count			
$\geq 1 \times 10^5/\mu L$	0.916	0.326–2.020	0.843
$<1 \times 10^5/\mu L$	1.000		
Prothrombin time			
≥77.5%	0.455	0.094–1.390	0.177
<77.5%	1.000		
Child-Pugh class			
A	1.464	0.539–6.813	0.493
B	1.000		
Spot-forming cells after treatment			
≥40	0.342	0.079–0.866	0.022
<40	1.000		

(hazard ratio 0.342, $P = 0.022$), as shown in Table 4. Therefore, the results suggest that TAA-specific CTLs detected after treatment are able to suppress the occurrence or recurrence of HCC in patients with no detectable HCCs after treatment.

Discussion

To determine whether TAA-specific CTLs suppress the occurrence or recurrence of HCC, we investigated the relationship between the magnitude of TAA-specific $CD8^+$ T-cell responses and the HCC-free interval in patients who had no detectable viable HCC 1 month after treatment for HCC. We found that potent TAA-specific $CD8^+$ T-cell responses, as observed 1 month after treatment for HCC, led to a prolonged HCC-free interval.

An HLA-A24-restricted MAGE-1 peptide-specific CTL line was established in a patient with metastatic melanoma [18], and an NY-ESO-1 DNA vaccine induced both antigen-specific effector $CD4^+$ and/or $CD8^+$ T-cell responses in most patients who did not show detectable pre-vaccination immune responses [19]. In addition, HLA-A2- and HLA-A24-restricted GPC3-derived peptide vaccine induced specific CTLs in mice [20]. In this study, we selected GPC3, MAGE-1, and NY-ESO-1 to monitor antigen-specific $CD8^+$ T-cell responses against HCC because they had been reported to be expressed commonly and frequently in HCC tissues [7, 11–13], and thus the combination of these TAAs would cover most HCCs. Among the 20 patients enrolled in the present study, 16 (80%) showed positive $CD8^+$ T-cell responses (10 or more SFCs) against the TAAs before and/or after the treatment. Although we did not examine the expression of TAAs in the HCC tissues, it would be expected that at least one of these three TAAs will be expressed in HCCs in patients who have a positive $CD8^+$ T-cell response against TAAs.

In patient 10, HCC recurrence was detected 3 months after treatment. Insufficient treatment or the pre-existence of intrahepatic metastases might be considered in a patient in whom HCCs are undetectable 1 month after treatment, but are detected within a few months after treatment. We expected that TAA-specific CTLs induced by treatment would suppress the development of a small HCC, which is not easily detected by conventional methods of examination. Thus, we enrolled and analyzed all patients in whom no HCC was detectable by ultrasonography, CT, and/or MRI 1 month after treatment, even if a recurrent or metastatic HCC was detected within a few months after treatment.

It is of interest whether tumor destruction by local HCC treatment would induce immune responses against HCCs. Apoptotic tumor cells are capable of inducing tumor-specific immune responses [21]. Dendritic cells, representing antigen-presenting cells, around damaged tumor cells take up tumor antigen released from the tumor cells and then migrate into draining lymph nodes [22]. There, they mature and stimulate tumor-specific helper T-cells and CTLs. In turn, the effector cells migrate into the tumor tissue and attack the tumor cells [23]. Tumor-specific immune responses were induced by a combination of direct dendritic cell injections into the HCC and radiation therapy that might induce tumor destruction [3]. When we compared TAA-specific $CD8^+$ T-cell responses before HCC treatment and those after treatment, about half of the patients (55%) showed an increased frequency of TAA-specific $CD8^+$ T-cells, which might have been induced by the treatment. However, the increase in TAA-specific CTLs did not affect the recurrence-free interval. Rather, it was the magnitude of TAA-specific $CD8^+$ T-cell responses after the treatment itself that affected the recurrence-free interval. Even if the frequency of these CTLs seemed to be decreased after treatment, they might infiltrate the liver. Furthermore, new CTLs other than pre-existing CTLs might be induced by the treatment because many TAA peptides recognized by CTLs were different between before and after the treatment. Although some patients showed a potent TAA-specific $CD8^+$ T-cell response before treatment, SFC before treatment did not correlate with the recurrence-free interval. We believe that TAA-specific CTLs are not able to control a large tumor burden by itself. As HCCs enlarge, they may secret immune suppressive factors such as TGF-β [24] and/or IL-10 [25] and modify gene expression of TAAs [26]. We speculate that TAA-specific CTLs detected after the treatment, but not detected before the treatment may be able to control HCCs. Otherwise, TAA-specific CTLs detected before the

treatment may be able to destroy a small HCC that was not detected by conventional examinations.

The ELISpot assay is a convenient means of detecting antigen-specific $CD8^+$ T-cells in a variety of diseases. We have detected HCV-specific $CD8^+$ T-cell responses in patients with acute HCV infection using this method and identified 6 new epitopes within the HCV protein [17]. In fact, we identified a novel GPC3-specific CTL epitope using this method (unpublished observation). At present, we are trying to identify more CTL epitopes among these TAAs that will be used as cancer vaccines.

In this study, we used peptide mixtures to stimulate $CD8^+$ T-cells. This procedure may mask responses to individual peptides because a peptide that interacts only weakly with HLA molecules is unable to attach to the molecule if the mixture contains 1 peptide with a high affinity for the same molecule. However, such a weak peptide would not contribute to tumor immune responses because of its weak interaction with the HLA molecules. Thus, we ignored this issue in this study.

Recurrence and multicentric carcinogenesis are major factors in determining the prognosis of HCC, and several treatments have been tried for the prevention of recurrence. IFN therapy [27, 28], treatment with acyclic retinoid therapy [29, 30], and adoptive immunotherapy [31] have been reported as effective in suppressing HCC recurrence. Preoperative hepatic function influenced early HCC recurrence in patients in whom small HCCs were resected [32]. This is consistent with our result that prothrombin time, reflecting hepatic function, affected the recurrence-free interval in the univariate analysis. In our study, higher platelet counts also contributed to a longer recurrence-free interval in the univariate analysis. In the multivariate analysis, however, only the magnitude of TAA-specific $CD8^+$ T-cell responses remained as an independent factor contributing to a longer recurrence-free interval.

Although the size and number of HCCs were reported to affect the period of HCC-free survival (recurrence) in patients with HCC treated by hepatic resection [33], they are not significant factors affecting the recurrence-free interval. Further investigation, such as the accumulation of analyses of HCC patients, is needed to clarify this issue. Sixteen out of 20 patients without detectable HCC 1 month after treatment had recurrent or metastatic HCCs during the observation period in this study. Our results suggest that the maintenance of strong TAA-specific $CD8^+$ T-cell responses for a long period may lead to a longer recurrence-free state. A long-term observation of TAA-specific immune responses should also be performed in any future study.

The results of our study suggest that strong TAA-specific $CD8^+$ T-cell responses would suppress HCC recurrence in patients with HCC who are treated by RFA or TACE and in whom any HCC is undetectable by ultrasonography, CT, and/or MRI 1 month after treatment. Since recurrence and intrahepatic metastasis are major risk factors influencing the prognosis of patients with HCC, immunotherapy to induce TAA-specific $CD8^+$ T-cells, such as a peptide vaccine, should be considered for clinical application in patients with HCC after local therapy.

Acknowledgments This study was supported in part by a grant from the Ministry of Health, Labor and Welfare of Japan (Kazumasa Hiroishi, Michio Imawari); a Grant-in-Aid for Scientific Research (C) from the Ministry of Education, Culture, Sports, Science and Technology of Japan (Kazumasa Hiroishi); and a grant for the High-Technology Research Center Project from the Ministry of Education, Culture, Sports, Science and Technology of Japan (Michio Imawari).

References

1. Palmer DH, Midgley RS, Mirza N, Torr EE, Ahmed F, Steele JC, et al. A phase II study of adoptive immunotherapy using dendritic cells pulsed with tumor lysate in patients with hepatocellular carcinoma. Hepatology. 2009;49:124–32.
2. Lee WC, Wang HC, Hung CF, Huang PF, Lia CR, Chen MF. Vaccination of advanced hepatocellular carcinoma patients with tumor lysate-pulsed dendritic cells: a clinical trial. J Immunother. 2005;28:496–504.
3. Chi KH, Liu SJ, Li CP, Kuo HP, Wang YS, Chao Y, et al. Combination of conformal radiotherapy and intratumoral injection of adoptive dendritic cell immunotherapy in refractory hepatoma. J Immunother. 2005;28:129–35.
4. van der Bruggen P, Traversari C, Chomez P, Lurquin C, De Plaen E, Van den Eynde B, et al. A gene encoding an antigen recognized by cytolytic T lymphocytes on a human melanoma. Science. 1991;254:1643–7.
5. Suzuki K, Tsujitani S, Konishi I, Yamaguchi Y, Hirooka Y, Kaibara N. Expression of MAGE genes and survival in patients with hepatocellular carcinoma. Int J Oncol. 1999;15:1227–32.
6. Tahara K, Mori M, Sadanaga N, Sakamoto Y, Kitano S, Makuuchi M. Expression of the MAGE gene family in human hepatocellular carcinoma. Cancer. 1999;85:1234–40.
7. Kariyama K, Higashi T, Kobayashi Y, Nouso K, Nakatsukasa H, Yamano T, et al. Expression of MAGE-1 and -3 genes and gene products in human hepatocellular carcinoma. Br J Cancer. 1999;81:1080–7.
8. Ueda Y, Shimizu K, Itoh T, Fuji N, Naito K, Shiozaki A, et al. Induction of peptide-specific immune response in patients with primary malignant melanoma of the esophagus after immunotherapy using dendritic cells pulsed with MAGE peptides. Jpn J Clin Oncol. 2007;37:140–5.
9. Chen YT, Scanlan MJ, Sahin U, Tureci O, Gure AO, Tsang S, et al. A testicular antigen aberrantly expressed in human cancers detected by autologous antibody screening. Proc Natl Acad Sci USA. 1997;94:1914–8.
10. Korangy F, Ormandy LA, Bleck JS, Klempnauer J, Wilkens L, Manns MP, et al. Spontaneous tumor-specific humoral and cellular immune responses to NY-ESO-1 in hepatocellular carcinoma. Clin Cancer Res. 2004;10:4332–41.
11. Chen CH, Chen GJ, Lee HS, Huang GT, Yang PM, Tsai LJ, et al. Expressions of cancer-testis antigens in human hepatocellular carcinomas. Cancer Lett. 2001;164:189–95.
12. Hsu HC, Cheng W, Lai PL. Cloning and expression of a developmentally regulated transcript MXR7 in hepatocellular

carcinoma: biological significance and temporospatial distribution. Cancer Res. 1997;57:5179–84.
13. Capurro M, Wanless IR, Sherman M, Deboer G, Shi W, Miyoshi E, et al. Glypican-3: a novel serum and histochemical marker for hepatocellular carcinoma. Gastroenterology. 2003;125:89–97.
14. Nakatsura T, Yoshitake Y, Senju S, Monji M, Komori H, Motomura Y, et al. Glypican-3, overexpressed specifically in human hepatocellular carcinoma, is a novel tumor marker. Biochem Biophys Res Commun. 2003;306:16–25.
15. Hippo Y, Watanabe K, Watanabe A, Midorikawa Y, Yamamoto S, Ihara S, et al. Identification of soluble NH2-terminal fragment of glypican-3 as a serological marker for early-stage hepatocellular carcinoma. Cancer Res. 2004;64:2418–23.
16. Shiina S, Teratani T, Obi S, Sato S, Tateishi R, Fujishima T, et al. A randomized controlled trial of radiofrequency ablation with ethanol injection for small hepatocellular carcinoma. Gastroenterology. 2005;129:122–30.
17. Doi H, Hiroishi K, Shimazaki T, Eguchi J, Baba T, Ito T, et al. Magnitude of CD8 T-cell responses against hepatitis C virus and severity of hepatitis do not necessarily determine outcomes in acute hepatitis C virus infection. Hepatol Res. 2009;39:256–65.
18. Akiyama Y, Maruyama K, Tai S, Komiyama M, Iizuka A, Takikawa M, et al. Characterization of a MAGE-1-derived HLA-A24 epitope-specific CTL line from a Japanese metastatic melanoma patient. Anticancer Res. 2009;29:647–55.
19. Gnjatic S, Altorki NK, Tang DN, Tu SM, Kundra V, Ritter G, et al. NY-ESO-1 DNA vaccine induces T-cell responses that are suppressed by regulatory T cells. Clin Cancer Res. 2009; 15:2130–9.
20. Motomura Y, Ikuta Y, Kuronuma T, Komori H, Ito M, Tsuchihara M, et al. HLA-A2 and -A24-restricted glypican-3-derived peptide vaccine induces specific CTLs: preclinical study using mice. Int J Oncol. 2008;32:985–90.
21. Albert ML, Sauter B, Bhardwaj N. Dendritic cells acquire antigen from apoptotic cells and induce class I-restricted CTLs. Nature. 1998;392:86–9.
22. Onaitis M, Kalady MF, Pruitt S, Tyler DS. Dendritic cell gene therapy. Surg Oncol Clin N Am. 2002;11:645–60.
23. Banchereau J, Steinman RM. Dendritic cells and the control of immunity. Nature. 1998;392:245–52.
24. Gastl G, Plante M, Finstad CL, Wong GY, Federici MG, Bander NH, et al. High IL-6 levels in ascitic fluid correlate with reactive thrombocytosis in patients with epithelial ovarian cancer. Br J Haematol. 1993;83:433–41.
25. Hersh EM, Stopeck AT. Advances in the biological therapy and gene therapy of malignant disease. Clin Cancer Res. 1997; 3:2623–9.
26. Cormier JN, Panelli MC, Hackett JA, Bettinotti MP, Mixon A, Wunderlich J, et al. Natural variation of the expression of HLA and endogenous antigen modulates CTL recognition in an in vitro melanoma model. Int J Cancer. 1999;80:781–90.
27. Ikeda K, Arase Y, Saitoh S, Kobayashi M, Suzuki Y, Suzuki F, et al. Interferon beta prevents recurrence of hepatocellular carcinoma after complete resection or ablation of the primary tumor-A prospective randomized study of hepatitis C virus-related liver cancer. Hepatology. 2000;32:228–32.
28. Kubo S, Nishiguchi S, Hirohashi K, Tanaka H, Shuto T, Yamazaki O, et al. Effects of long-term postoperative interferon-alpha therapy on intrahepatic recurrence after resection of hepatitis C virus-related hepatocellular carcinoma. A randomized, controlled trial. Ann Intern Med. 2001;134:963–7.
29. Muto Y, Moriwaki H, Ninomiya M, Adachi S, Saito A, Takasaki KT, et al. Prevention of second primary tumors by an acyclic retinoid, polyprenoic acid, in patients with hepatocellular carcinoma. Hepatoma Prevention Study Group. N Engl J Med. 1996; 334:1561–7.
30. Muto Y, Moriwaki H, Saito A. Prevention of second primary tumors by an acyclic retinoid in patients with hepatocellular carcinoma. N Engl J Med. 1999;340:1046–7.
31. Takayama T, Sekine T, Makuuchi M, Yamasaki S, Kosuge T, Yamamoto J, et al. Adoptive immunotherapy to lower postsurgical recurrence rates of hepatocellular carcinoma: a randomised trial. Lancet. 2000;356:802–7.
32. Kaibori M, Ishizaki M, Saito T, Matsui K, Kwon AH, Kamiyama Y. Risk factors and outcome of early recurrence after resection of small hepatocellular carcinomas. Am J Surg. 2009;198:39–45.
33. Maeda T, Shimada M, Harimoto N, Tsujita E, Aishima S, Tanaka S, et al. Prognosis of early hepatocellular carcinoma after hepatic resection. Hepatogastroenterology. 2008;55:1428–32.

HEPATOLOGY
Official Journal of the American Association for the Study of Liver Diseases

Discrete Nature of EpCAM$^+$ and CD90$^+$ Cancer Stem Cells in Human Hepatocellular Carcinoma

Taro Yamashita,[1] Masao Honda,[1] Yasunari Nakamoto,[1] Masayo Baba,[1] Kouki Nio,[1] Yasumasa Hara,[1] Sha Sha Zeng,[1] Takehiro Hayashi,[1] Mitsumasa Kondo,[1] Hajime Takatori,[1] Tatsuya Yamashita,[1] Eishiro Mizukoshi,[1] Hiroko Ikeda,[1] Yoh Zen,[1] Hiroyuki Takamura,[1] Xin Wei Wang,[2] and Shuichi Kaneko[1]

Recent evidence suggests that hepatocellular carcinoma (HCC) is organized by a subset of cells with stem cell features (cancer stem cells; CSCs). CSCs are considered a pivotal target for the eradication of cancer, and liver CSCs have been identified by the use of various stem cell markers. However, little information is known about the expression patterns and characteristics of marker-positive CSCs, hampering the development of personalized CSC-targeted therapy. Here, we show that CSC markers EpCAM and CD90 are independently expressed in liver cancer. In primary HCC, EpCAM$^+$ and CD90$^+$ cells resided distinctively, and gene-expression analysis of sorted cells suggested that EpCAM$^+$ cells had features of epithelial cells, whereas CD90$^+$ cells had those of vascular endothelial cells. Clinicopathological analysis indicated that the presence of EpCAM$^+$ cells was associated with poorly differentiated morphology and high serum alpha-fetoprotein (AFP), whereas the presence of CD90$^+$ cells was associated with a high incidence of distant organ metastasis. Serial xenotransplantation of EpCAM$^+$/CD90$^+$ cells from primary HCCs in immunedeficient mice revealed rapid growth of EpCAM$^+$ cells in the subcutaneous lesion and a highly metastatic capacity of CD90$^+$ cells in the lung. In cell lines, CD90$^+$ cells showed abundant expression of c-Kit and *in vitro* chemosensitivity to imatinib mesylate. Furthermore, CD90$^+$ cells enhanced the motility of EpCAM$^+$ cells when cocultured *in vitro* through the activation of transforming growth factor beta (TGF-β) signaling, whereas imatinib mesylate suppressed *TGFB1* expression in CD90$^+$ cells as well as CD90$^+$ cell-induced motility of EpCAM$^+$ cells. *Conclusion*: Our data suggest the discrete nature and potential interaction of EpCAM$^+$ and CD90$^+$ CSCs with specific gene-expression patterns and chemosensitivity to molecular targeted therapy. The presence of distinct CSCs may determine the clinical outcome of HCC. (HEPATOLOGY 2012;00:000–000)

The cancer stem cell (CSC) hypothesis, which suggests that a subset of cells bearing stem-cell–like features is indispensable for tumor development, has recently been put forward subsequent to advances in molecular and stem cell biology. Liver cancer, including hepatocellular carcinoma (HCC), is a leading cause of cancer death worldwide.[1] Recent studies have shown the existence of CSCs in liver cancer cell lines and primary HCC specimens using various stem cell markers.[2-7] Independently, we have identified novel HCC subtypes defined by the hepatic stem/progenitor cell markers,

Abbreviations: 5-FU, fluorouracil; Abs, antibodies; AFP, alpha-fetoprotein; CK-19, cytokeratin-19; CSC, cancer stem cell; DNs, dysplastic nodules; EMT, epithelial mesenchymal transition; EpCAM; epithelial cell adhesion molecule; FACS, fluorescent-activated cell sorting; HBV, hepatitis B virus; HCC, hepatocellular carcinoma; HCV, hepatitis C virus; HSCs, hepatic stem cells; IF, immunofluorescence; IHC, immunohistochemistry; IR, immunoreactivity; MDS, multidimensional scaling; NBNC, non-B, non-C hepatitis; NOD/SCID, nonobese diabetic, severe combined immunodeficient; NT, nontumor; OV-1, ovalbumin 1; qPCR, quantitative real-time polymerase chain reaction; SC, subcutaneous; Smad3, Mothers against decapentaplegic homolog 3; TECs, tumor epithelial cells; TGF-β, transforming growth factor beta; T/N, tumor/nontumor; VECs, vascular endothelial cells; VM, vasculogenic mimicry; VEGFR, vascular endothelial growth factor receptor.

From the [1]Liver Center, Kanazawa University Hospital, Kanazawa, Ishikawa, Japan; and [2]Laboratory of Human Carcinogenesis, Center for Cancer Research, National Cancer Institute, Bethesda, MD.

Received July 9, 2012; revised October 22, 2012; accepted November 6, 2012.

This study was supported by a Grant-in-Aid from the Ministry of Education, Culture, Sports, Science, and Technology of Japan (23590967), a grant from the Japanese Society of Gastroenterology, a grant from the Ministry of Health, Labor, and Welfare, and a grant from the National Cancer Center Research and Development Fund (23-B-5) of Japan. X.W.W. is supported by the Intramural Research Program of the Center for Cancer Research, U.S. National Cancer Institute.

epithelial cell adhesion molecule (EpCAM) and alpha-fetoprotein (AFP), which correlate with distinct gene-expression signatures and prognosis.[8,9] $EpCAM^+$ HCC cells isolated from primary HCC and cell lines show CSC features, including tumorigenicity, invasiveness, and resistance to fluorouracil (5-FU).[10] Similarly, other groups have shown that $CD133^+$, $CD90^+$, and $CD13^+$ HCC cells are also CSCs, and that EpCAM, CD90, and CD133 are the only markers confirmed to enrich CSCs from primary HCCs thus far.[3-5,10]

Although $EpCAM^+$, $CD90^+$, and $CD133^+$ cells show CSC features, such as high tumorigenicity, an invasive nature, and resistance to chemo- and radiation therapy, it remains unclear whether these cells represent an identical HCC population and whether they share similar or distinct characteristics. In this study, we used fluorescent-activated cell sorting (FACS), microarray, and immunohistochemistry (IHC) techniques to investigate the expression patterns of the representative liver CSC markers CD133, CD90, and EpCAM in a total of 340 HCC cases and 7 cases of mesenchymal liver tumors. We further explored gene- and protein-expression patterns as well as tumorigenic capacity of sorted cells isolated from 15 primary HCCs and 7 liver cancer cell lines in an attempt to identify the molecular portraits of each cell type.

Materials and Methods

Clinical Specimens. HCC samples were obtained with informed consent from patients who had undergone radical resection at the Liver Center in Kanazawa University Hospital (Kanazawa, Japan), and tissue acquisition procedures were approved by the ethics committee of Kanazawa University. A total of 102 formalin-fixed and paraffin-embedded HCC samples, obtained from 2001 to 2007, were used for IHC analyses. Fifteen fresh HCC samples were obtained between 2008 and 2012 from surgically resected specimens and an autopsy specimen and were used immediately to prepare single-cell suspensions and xenotransplantation (Table 1). Seven hepatic stromal tumors (three cavernous hemangioma, two hemangioendothelioma, and two angiomyolipoma) were formalin fixed and paraffin embedded and used for IHC analyses.

Table 1. Clinicopathological Characteristics of HCC Cases Used for Xenotransplantation

ID	Age/ Sex	Etiology	Tumor Size (cm)	Histological Grade	AFP (ng/mL)	DCP (IU/mL)
P1	77/M	Alcohol	12.0	Moderate	198	322
P2	61/F	NBNC	11.0	Moderate	12	3,291
P3	66/M	NBNC	2.2	Moderate	13	45
P4	65/M	HCV	4.2	Poor	13,700	25,977
P5	52/M	HBV	6.0	Moderate	29,830	1,177
P6	60/M	HCV	2.7	Poor	249	185
P7	79/F	HBV	4.0	Poor	46,410	384
P8	77/F	NBNC	5.5	Moderate	17,590	562
P9	71/M	Alcohol	7.0	Poor	3,814	607
P10	51/M	HBV	2.2	Well	<10	21
P11	71/M	Alcohol	2.1	Well	<10	11
P12	60/M	HBV	10.8	Poor	323	2,359
P13	66/M	HCV	2.8	Moderate	11	29
P14	71/M	HCV	7.2	Moderate	235,700	375,080
P15	75/M	HBV	5.5	Poor	<10	97

Abbreviation: DCP, des-gamma-carboxy prothrombin.

Additional details of experimental procedures are available in the Supporting Information.

Results

EpCAM, CD133, and CD90 Expression in HCC. We first evaluated the frequencies of three representative CSC markers ($EpCAM^+$, $CD90^+$, and $CD133^+$ cells) in 12 fresh primary HCC cases surgically resected by FACS (representative data shown in Fig. 1A). Clinicopathological characteristics of primary HCC cases are shown in Table 1. We noted that frequency of $EpCAM^+$, $CD90^+$, and $CD133^+$ cells varied between individuals. Abundant $CD90^+$ (7.0%), but almost no $EpCAM^+$, cells (0.06%, comparable to the isotype control) were detected in P2, whereas few $CD90^+$ (0.6%), but abundant $EpCAM^+$, cells (17.5%) were detected in P4. Very small populations of $EpCAM^+$ (0.09%), $CD90^+$ (0.04%), and $CD133^+$ cells (0.05%) were found in P12, but they were almost nonexistent in P8, except for $CD90^+$ cells (0.08%) (Fig. 1A). We further evaluated the expression of EpCAM, CD90, and CD133 in xenografts obtained from surgically resected samples (P13 and P15) and an autopsy sample (P14). As a whole, compared to the isotype control, 7 of 15 HCCs contained definite $EpCAM^+$ cells (46.7%), whereas only 3 HCCs

Address reprint requests to: Taro Yamashita, M.D., Ph.D., Department of General Medicine, Kanazawa University Hospital, 13-1 Takara-Machi, Kanazawa, Ishikawa 920-8641, Japan. E-mail: taroy@m-kanazawa.jp; fax: +81-76-234-4250.

View this article online at wileyonlinelibrary.com.
DOI 10.1002/hep.26168
Potential conflict of interest: Nothing to report.
Additional Supporting Information may be found in the online version of this article.

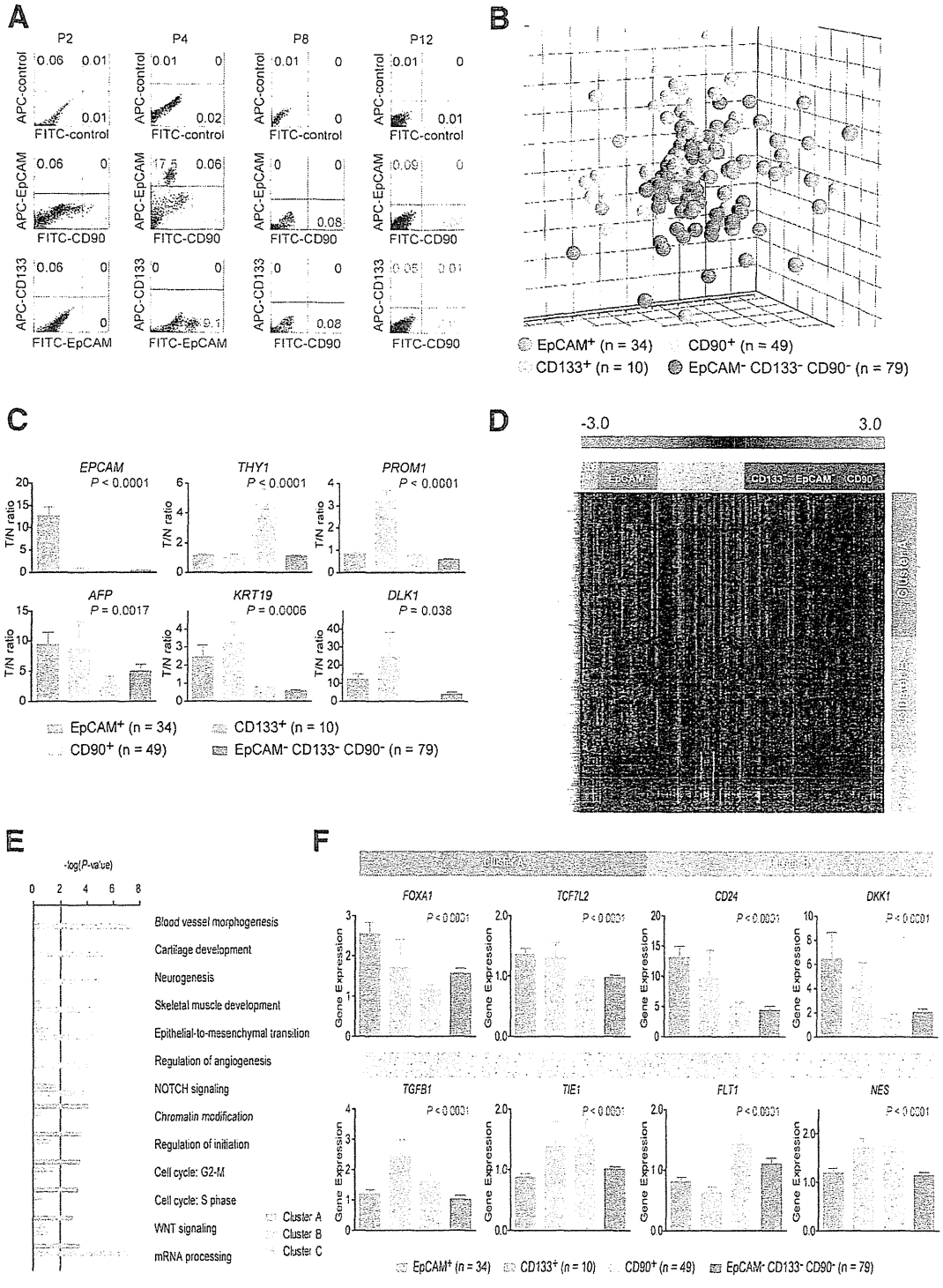

Fig. 1. Gene-expression profiles of CSC marker-positive HCCs. (A) FACS analysis of primary HCCs stained with fluorescent-labeled Abs against EpCAM, CD90, or CD133. (B) Multidimensional scaling analysis of 172 HCC cases characterized by the expression patterns of EpCAM, CD133, and CD90. Red, $EpCAM^+$ $CD90^-$ $CD133^-$ (n = 34); orange, $EpCAM^-$ $CD90^-$ $CD133^+$ (n = 10); light blue, $EpCAM^-$ $CD90^+$ $CD133^-$ (n = 49); blue, $EpCAM^-$ $CD90^-$ $CD133^-$ (n = 79). HCC specimens were clustered in specific groups with statistical significance ($P < 0.001$). (C) Expression patterns of well-known hepatic stem/progenitor markers in each HCC subtype, as analyzed by microarray. Red bar, $EpCAM^+$; orange bar, $CD133^+$; light blue bar, $CD90^+$; blue bar, $EpCAM^-$ $CD90^-$ $CD133^-$. (D) Hierarchical cluster analysis based on 1,561 EpCAM/CD90/CD133-coregulated genes in 172 HCC cases. Each cell in the matrix represents the expression level of a gene in an individual sample. Red and green cells depict high and low expression levels, respectively, as indicated by the scale bar. (E) Pathway analysis of EpCAM/CD90/CD133-coregulated genes. Canonical signaling pathways activated in cluster A (red bar), cluster B (orange bar), or cluster C (light blue bar) with statistical significance ($P < 0.01$) are shown. (F) Expression patterns of representative genes differentially expressed in EpCAM/CD90/CD133 HCC subtypes. Red bar, $EpCAM^+$; orange bar, $CD133^+$; light blue bar, $CD90^+$; blue bar, $EpCAM^-$ $CD133^-$ $CD90^-$.

Table 2. Tumorigenic Capacity of Unsorted, EpCAM$^+$, EpCAM$^-$, CD90$^+$, and CD90$^-$ Cells From Primary HCCs and Xenografts

Sample	CD133 (%)	CD90 (%)	EpCAM (%)	Cell Surface Marker	Number of Cells	Tumor Formation 2M	Tumor Formation 3M
P1	0	3.1	0	Unsorted	1×10^7	0/5	0/5
				CD90$^+$	1×10^5	0/5	0/5
				CD90$^-$	1×10^5	0/5	0/5
P2	0.06	7.0	0.06	Unsorted	1×10^7	0/5	0/5
				CD90$^+$	1×10^5	0/5	0/5
				CD90$^-$	1×10^5	0/5	0/5
P3	0	1.3	0	Unsorted	1×10^6	0/2	0/2
				CD90$^+$	1×10^4	0/4	0/4
				CD90$^-$	1×10^4	0/4	0/4
P4	0	0.6	17.5	Unsorted	1×10^6	3/4	4/4
				EpCAM$^+$	1×10^3	0/3	2/3
					1×10^4	3/4	4/4
					1×10^5	3/3	3/3
				CD90$^+$	1×10^3	0/3	0/3
					1×10^4	0/4	0/4
					1×10^5	0/3	0/3
				EpCAM$^-$ CD90$^-$	1×10^3	0/3	0/3
					1×10^4	0/4	0/4
					1×10^5	0/3	0/3
P5	0	0.8	29.7	Unsorted	1×10^6	0/5	0/5
				EpCAM$^+$	1×10^5	0/5	0/5
				CD90$^+$	1×10^5	0/5	0/5
				EpCAM$^-$ CD90$^-$	1×10^5	0/5	0/5
P6	0	0.7	0	Unsorted	1×10^6	0/2	0/2
				CD90$^+$	1×10^4	0/4	0/4
				CD90$^-$	1×10^4	0/4	0/4
P7	1.38	4.5	4.4	Unsorted	1×10^6	2/2	2/2
				EpCAM$^+$	2×10^2	0/3	0/3
					1×10^3	0/3	1/3
					1×10^4	2/4	4/4
				CD90$^+$	2×10^2	0/3	0/3
					1×10^3	0/3	0/3
					1×10^4	0/4	0/4
				EpCAM$^-$ CD90$^-$	1×10^3	0/3	0/3
					1×10^4	0/3	0/3
					1×10^5	0/4	0/4
P8	0	0.08	0	Unsorted	1×10^5	0/4	0/4
				CD90$^+$	1×10^3	0/3	0/3
				CD90$^-$	1×10^5	0/3	0/3
P9	0	0.26	0	Unsorted	1×10^5	0/4	0/4
				CD90$^+$	1×10^3	0/3	0/3
				CD90$^-$	1×10^5	0/3	0/3
P10	0	0.78	0	Unsorted	1×10^4	0/4	0/4
				CD90$^+$	1×10^3	0/3	0/3
				CD90$^-$	1×10^4	0/3	0/3
P11	0	0.1	1.54	Unsorted	5×10^4	0/2	0/2
				EpCAM$^+$	1×10^3	0/3	0/3
				CD90$^+$	1×10^3	0/3	0/3
				EpCAM$^-$ CD90$^-$	1×10^4	0/3	0/3
P12	0.06	0.05	0.09	Unsorted	1×10^5	0/3	3/3
				CD90$^+$	1×10^3	0/4	1/4
				CD90$^-$	1×10^3	0/4	1/4
					1×10^4	0/3	3/3
P13	0	0.03	67.7	EpCAM$^+$	5×10^5	4/4	NA
					5×10^4	3/3	NA
					5×10^3	3/3	NA
				EpCAM$^-$	5×10^5	0/4	NA
					5×10^4	0/3	NA
					5×10^3	0/3	NA
P14	24.0	0.06	3.1	EpCAM$^+$	5×10^3	4/5	NA
				EpCAM$^-$	5×10^3	2/5	NA
P15	0	2.45	0	CD90$^+$	5×10^4	3/4	NA
					5×10^3	1/3	NA
					5×10^2	1/3	NA
				CD90$^-$	5×10^4	2/4	NA
					5×10^3	1/3	NA
					5×10^2	0/3	NA

NA, not available.

contained definite CD133$^+$ cells (20%) (Table 2). CD90$^+$ cells were detected at variable frequencies in all 15 HCCs analyzed.

To explore the status of these CSC marker-positive cells in HCC in a large cohort, we utilized oligo-DNA microarray data from 238 HCC cases (GEO accession no.: GSE5975) to evaluate the expression of *EPCAM* (encoding EpCAM and CD326), *THY1* (encoding CD90), and *PROM1* (encoding CD133) in whole HCC tissues and nontumor (NT) tissues. Because previous studies demonstrated that CD133$^+$ and CD90$^+$ cells were detected at low frequency (~13.6% by CD133 staining and ~6.2% by CD90 staining) in HCC, but were almost nonexistent in NT liver (4, 5),[4,5] we utilized tumor/nontumor (T/N) gene-expression ratios to detect the existence of marker-positive CSCs in tumor. Accordingly, we showed that a 2-fold cutoff of T/N ratios of *EPCAM* successfully stratifies HCC samples with EpCAM$^+$ liver CSCs.[9,10]

A total of 95 (39.9%), 110 (46.2%), and 31 (13.0%) of the 238 HCC cases were thus regarded as EpCAM$^+$, CD90$^+$, and CD133$^+$ HCCs (T/N ratios: $\geq$2.0), respectively. As observed in the FACS data described above, we detected coexpression of EpCAM and CD90 in 45 HCCs (18.9%), EpCAM and CD133 in five HCCs (2%), CD90 and CD133 in five HCCs (2%), and EpCAM, CD90, and CD133 in 11 HCCs (4.6%). To clarify the characteristics of gene-expression signatures specific to stem cell marker expression status, we selected 172 HCC cases expressing a single CSC marker (34 EpCAM$^+$ CD90$^-$ CD133$^-$, 49 EpCAM$^-$ CD90$^+$ CD133$^-$, and 10 EpCAM$^-$ CD90$^-$ CD133$^+$) or all marker-negative HCCs (79 EpCAM$^-$ CD90$^-$ CD133$^-$). A class-comparison analysis with

univariate F tests and a global permutation test (×10,000) yielded a total of 1,561 differentially expressed genes. Multidimensional scaling (MDS) analysis using this gene set indicated that HCC specimens were clustered in specific groups with statistical significance ($P < 0.001$). Close examination of MDS plots revealed three major HCC subtype clusters: all marker-negative HCCs (blue spheres); EpCAM single-positive HCCs (red spheres); and CD90 single-positive HCCs (light blue spheres). $CD133^+$ HCCs (orange spheres) were rare, relatively scattered, and not clustered (Fig. 1B).

We examined the expression of representative hepatic stem/progenitor cell markers *AFP*, *KRT19*, and *DLK1* in HCCs with regard to the gene-expression status of each CSC marker (Fig. 1C). All three markers were up-regulated in $EpCAM^+$ and $CD133^+$ HCCs, compared with all marker-negative HCCs, consistent with previous findings.[10,11] However, we found no significant overexpression of *AFP*, *KRT19*, and *DLK1* in $CD90^+$ and all marker-negative HCCs.

Hierarchical cluster analyses revealed three main gene clusters that were up-regulated in $EpCAM^+$ HCCs (cluster A, 706 genes), $EpCAM^+$ or $CD133^+$ HCCs (cluster B, 530 genes), and $CD90^+$ or $CD133^+$ HCCs (cluster C, 325 genes) (Fig. 1D). Pathway analysis indicated that the enriched genes in cluster A (red bar) were associated with chromatin modification, cell-cycle regulation, and Wnt/β-catenin signaling (Fig. 1E). Genes associated with messenger RNA processing were enriched in clusters A (red bar) and B (orange bar). Surprisingly, genes in cluster C were significantly associated with pathways involved in blood-vessel morphogenesis, angiogenesis, neurogenesis, and epithelial mesenchymal transition (EMT) (light blue bar). Close examination of genes in each cluster suggested that known hepatic transcription factors (*FOXA1*), Wnt regulators (*TCF7L2* and *DKK1*), and a hepatic stem cell marker (*CD24*) were dominantly up-regulated in $EpCAM^+$ and $CD133^+$ HCCs (Fig. 1F). By contrast, genes associated with blood-vessel morphogenesis (*TIE1* and *FLT1*), EMT (*TGFB1*), and neurogenesis (*NES*) were activated dominantly in $CD90^+$ HCCs and $CD133^+$ HCCs.

$CD90^+$ HCC Cells Share Features With Mesenchymal Vascular Endothelial Cells. Because $CD133^+$ HCCs were relatively rare and constituted only 13% (microarray cohort) to 20% (FACS cohort) of all HCC samples analyzed, we focused on the characterization of EpCAM and CD90. To clarify the cell identity of $EpCAM^+$ or $CD90^+$ cells in primary HCCs, we performed IHC analysis of 18 needle-biopsy specimens of premalignant dysplastic nodules (DNs), 102 surgically resected HCCs, and corresponding NT liver tissues. When examining the expression of EpCAM and CD90 in cirrhotic liver tissue by double-color IHC analysis, we found that $EpCAM^+$ cells and $CD90^+$ cells were distinctively located and not colocalized (Supporting Fig. 1A). Immunoreactivity (IR) to anti-CD90 antibodies (Abs) was detected in vascular endothelial cells (VECs), inflammatory cells, fibroblasts, and neurons, but not in hepatocytes or cholangiocytes, in the cirrhotic liver (Supporting Fig. 1B, panels a,b). IR to anti-EpCAM Abs was detected in hepatic progenitors adjacent to the periportal area and bile duct epithelial cells in liver cirrhosis (Supporting Fig. 1B, panels c,d).

IR to anti-EpCAM Abs was detected in 37 of 102 surgically resected HCCs (Fig. 2A, panel b), but not in 18 DNs (Fig. 2A, panel a). By contrast, no tumor epithelial cells (TECs) showing IR to anti-CD90 Abs were found in any of the 18 DNs or 102 HCCs examined (Fig. 2A, panels c,d). However, we identified $CD90^+$ cells that were morphologically similar to VECs or fibroblasts within the tumor nodule in 37 of the 102 surgically resected HCC tissues (≥5% positive staining in a given area). IR to anti-CD90 Abs was also detected in hepatic mesenchymal tumors (Supporting Fig. 1C, panels a-c), indicating that CD90 is also a marker of liver stromal tumors.

Double-color IHC and immunofluorescence (IF) analysis confirmed the distinct expression of EpCAM and CD90 in HCC (Fig. 2B), consistent with the FACS data (Fig. 1A). Quantitative real-time polymerase chain reaction (qPCR) analysis of sorted $EpCAM^+$, $CD90^+$, and $EpCAM^-$ $CD90^-$ cells after $CD45^+$ cell depletion indicated that the hepatic stem/progenitor markers, *AFP* and *KRT19*, were up-regulated in $EpCAM^+$ cells (red bar), whereas the mesenchymal markers, *KIT* and *FLT1*, were up-regulated in $CD90^+$ cells (orange bar), compared with $EpCAM^-$ $CD90^-$ cells (blue bar) (Fig. 2C). The hepatocyte marker, *CYP3A4*, was down-regulated in $EpCAM^+$ cells and not detected in $CD90^+$ cells, compared with $EpCAM^-$ $CD90^-$ cells. *POU5F1* and *BMI1* were equally up-regulated in both $EpCAM^+$ and $CD90^+$ cells, compared with $EpCAM^-$ $CD90^-$ cells.

EpCAM and CD90 were independently and distinctively expressed in different cellular lineages, so we evaluated the staining of EpCAM and CD90 separately and analyzed the clinicopathological characteristics of surgically resected HCC cases. HCCs were regarded marker positive if ≥5% positive staining was detected in a given area. The existence of $EpCAM^+$

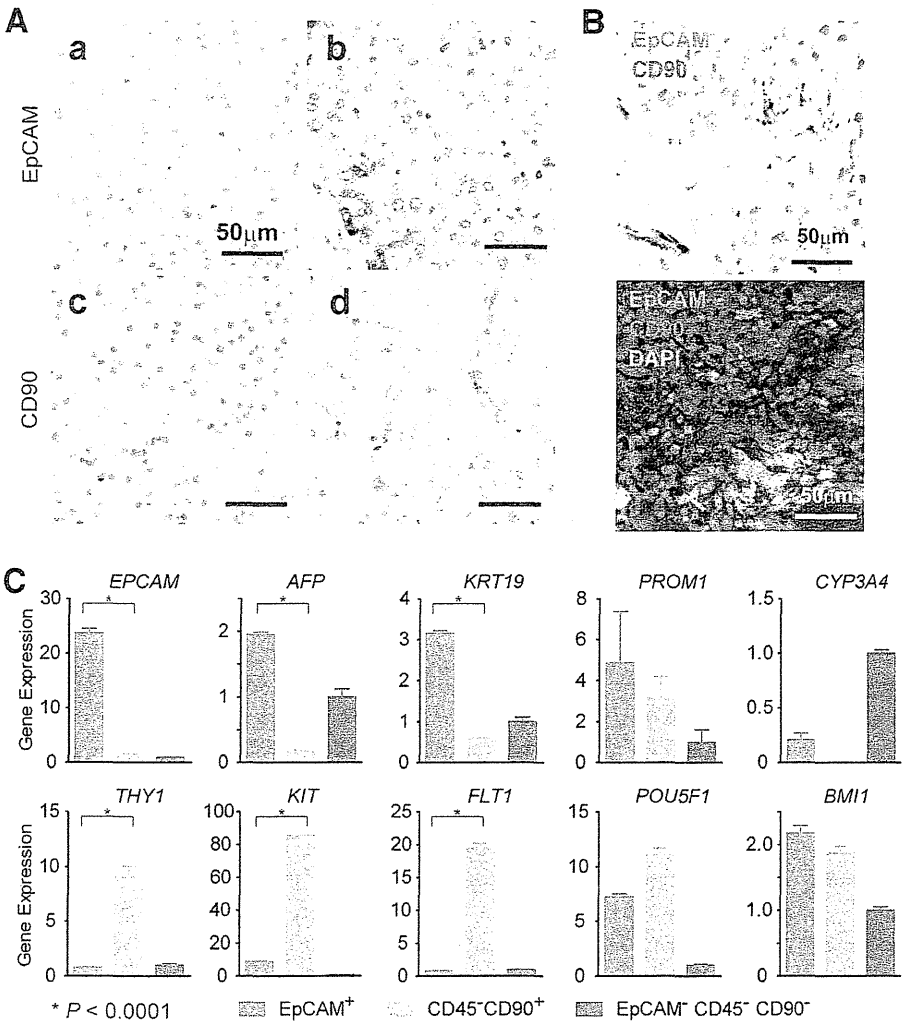

Fig. 2. Distinct EpCAM$^+$ and CD90$^+$ cell populations in HCC. (A) Representative images of EpCAM and CD90 staining in dysplastic nodule (panels a,c) and HCC (panels b,d) by IHC analysis (scale bar, 50 μm). EpCAM (panels a,b) and CD90 (panels c,d) immunostaining is depicted. (B) Upper panel: representative images of EpCAM (red) and CD90 (brown) double staining in HCC by IHC (scale bar, 50 μm). Lower panel: representative images of EpCAM (green) and CD90 (red) staining with 4'6-diamidino-phenylindole (DAPI) (blue) in HCC by IF (scale bar, 50 μm). (C) qPCR analysis of sorted EpCAM$^+$ (red bar), CD90$^+$ (orange bar), or EpCAM$^-$ CD90$^-$ (blue bar) derived from a representative primary HCC. Experiments were performed in triplicate, and data are shown as mean ± standard error of the mean.

cells (≥5%) was characterized by poorly differentiated morphology and high serum AFP values with a tendency for portal vein invasion, whereas the existence of CD90$^+$ cells (≥5%) was associated with poorly differentiated morphology and a tendency for large tumor size (Supporting Tables 2 and 3). Notably, the existence of CD90$^+$ cells was associated with a high incidence of distant organ metastasis, including lung, bone, and adrenal gland, within 2 years after surgery, whereas EpCAM$^+$ cell abundance appeared unrelated to distant organ metastasis.

We evaluated the characteristics of EpCAM$^+$ or CD90$^+$ cells in seven representative HCC cell lines. Morphologically, all EpCAM$^+$ cell lines (HuH1, HuH7, and Hep3B) showed a polygonal, epithelial cell shape, whereas three of four CD90$^+$ cell lines (HLE, HLF, and SK-Hep-1) showed a spindle cell shape (Fig. 3A). EpCAM$^+$ cells were detected in 11.5%, 57.7%, and 99.6% of sorted HuH1, HuH7, and Hep3B cells, respectively. A small CD90$^+$ cell population (0.66%) was observed in PLC/PRL/5, whereas 91.3%, 10.8%, and 59.0% of CD90$^+$ cells were detected in HLE, HLF, and SK-Hep-1, respectively. Compared with primary HCCs, only EpCAM$^+$ or CD90$^+$ cells were detected in liver cancer cell lines under normal culture conditions (Fig. 3B), suggesting that these cell lines contain a relatively pure cell population most likely obtained by clonal selection through the establishment process.

A class-comparison analysis with univariate *t* tests and a global permutation test (×10,000) of microarray data yielded two main gene clusters up-regulated in EpCAM$^+$ cell lines (HuH1, HuH7, and Hep3B) (cluster I, 524 genes) or in CD90$^+$ cell lines (HLE, HLF, and SK-Hep-1) (cluster II, 366 genes) (Fig. 3C). PLC/PRL/5 showed intermediate gene-expression patterns between EpCAM$^+$ and CD90$^+$ cell lines using this gene set. Pathway analysis indicated that the genes

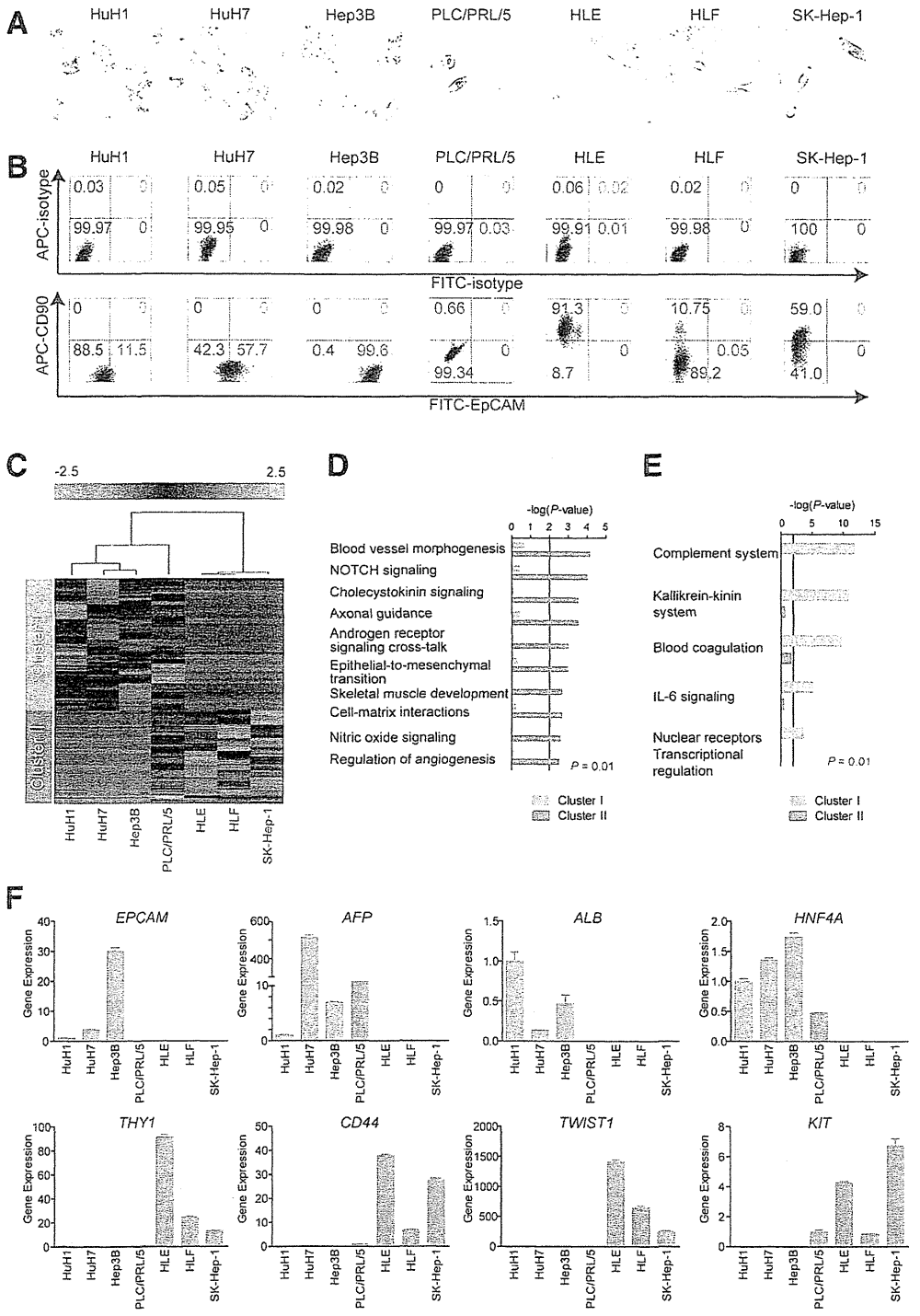

Fig. 3. Characteristics of HCC cell lines defined by EpCAM and CD90. (A) Representative photomicrographs of $EpCAM^{+}CD90^{-}$ and $EpCAM^{-}$ $CD90^{+}$ HCC cell lines. (B) Representative FACS data of $EpCAM^{+}CD90^{-}$ and $EpCAM^{-}$ $CD90^{+}$ HCC cell lines stained with fluorescein isothiocyanate (FITC)-EpCAM and APC-CD90 Abs. (C) Heat-map images of seven HCC cell lines based on 890 EpCAM/CD90-coregulated genes. Each cell in the matrix represents the expression level of a gene in an individual sample. Red and green cells depict high and low expression levels, respectively, as indicated by the scale bar. (D and E) Pathway analysis of EpCAM/CD90-coregulated genes. Canonical signaling pathways activated in cluster I (orange bar) or II (blue bar) with statistical significance ($P < 0.01$) are shown. (F) qPCR of representative differentially expressed genes identified by microarray analysis (C) in seven HCC cell lines.

enriched in cluster II were mainly associated with blood-vessel morpho- and angiogenesis (Fig. 3D). By contrast, the enriched genes in cluster I were significantly associated with known hepatocyte functions ($P < 0.01$) (Fig. 3E). In addition, we identified that the enriched genes in cluster II were significantly associated with neurogenesis, skeletal muscle development, and EMT.

We used qPCR to validate that known hepatic stem cell (HSC) and hepatocyte markers, such as *AFP, EPCAM, ALB*, and *HNF4A* genes, were up-regulated in $EpCAM^+$ cell lines, but not detected in $CD90^+$ cell lines (Fig. 3F). By contrast, genes associated with mesenchymal lineages and EMT, such as *KIT, TWIST1, CD44*, and *THY1*, were strongly up-regulated in $CD90^+$ cell lines.

Unique Tumorigenicity and Metastasis Capacity of Distinct CSCs Defined by EpCAM and CD90. We investigated the tumorigenic capacity of $EpCAM^+$ or $CD90^+$ cells by subcutaneously (SC) injecting 1×10^5 sorted cells of four HCC cell lines (HuH1, HuH7, HLE, and HLF) into nonobese diabetic, severe combined immunodeficient (NOD/SCID) mice. We excluded Hep3B cells for the evaluation of tumorigenicity because almost 100% of cells were EpCAM positive. We further excluded SK-Hep-1 cells from the analysis because they potentially originated from endothelial cells.[12] The highly tumorigenic capacities of $EpCAM^+$ and $CD90^+$ cells were reproduced in HuH1, HuH7, and HLF cell lines, compared with marker-negative cells (Fig. 4A). However, HLE cells did not produce SC tumors, even 12 months after transplantation, in NOD/SCID mice. $EpCAM^+$ cells from HuH1 and HuH7 formed larger tumors more rapidly than $CD90^+$ cells from HLF (Fig. 4B). IHC analyses indicated that $EpCAM^+$ cells did not produce $CD90^+$ cells and *vice versa* in these cell lines *in vivo* (Fig. 4C). $CD90^+$ cells showed a high metastatic capacity, whereas $EpCAM^+$ cells showed no metastasis to the lung when SC tumor volume reached approximately 2,000 (HuH1 and HuH7) or 700 mm^3 (HLF) (Fig. 4D). The high metastatic capacity of PLC/PRL/5 cells, which contain a small population of $CD90^+$ cells, was also confirmed after SC injection into NOD/SCID mice (data not shown). $CD90^+$ cells could divide to generate both $CD90^+$ and $CD90^-$ cells, and $CD90^+$ cells showed a high capacity to invade and form spheroids with overexpression of *TWIST1* and *TWIST2*, which are known to activate EMT programs in HLF cells (Supporting Fig. 2A-D).

We next evaluated the tumorigenic/metastatic capacity of $CD45^-$ tumor cells using 12 fresh primary HCC specimens (P1-P12) that had been surgically resected (Table 2). We further evaluated the tumorigenicity of EpCAM/CD90 sorted cells obtained from xenografts derived from primary HCCs (Supporting Fig. 3A). Of these, we confirmed the tumorigenicity of cancer cells obtained from six primary HCCs after SC injection into NOD/SCID mice within 3 months after transplantation (Fig. 5A; Table 2; Supporting Fig. 3B). $EpCAM^+$ cells derived from four HCCs (P4, P7, P13, and P14) showed highly tumorigenic capacities, compared with $EpCAM^-$ cells. $CD90^+$ cells derived from two HCCs showed equal (P12) or more-tumorigenic capacities (P15), compared with $CD90^-$ cells. Tumorigenicity of $EpCAM^+$ cells was observed in three hepatitis C virus (HCV)-related HCCs and an hepatitis B virus (HBV)-related HCC, whereas tumorigenicity of $CD90^+$ cells was observed in two HBV-related HCCs (Tables 1 and 2).

Using unsorted cells, we compared the frequency of $EpCAM^+$ and $CD90^+$ cells in primary and xenograft tumors and found that $EpCAM^+$ cells remained, but $CD90^+$ cells disappeared, in secondary tumors derived from P4 or P7, whereas $EpCAM^+$ cells disappeared, but $CD90^+$ cells remained, in secondary tumors derived from P12 (Fig. 5B). Morphologically, tumorigenic $EpCAM^+$ cells showed an epithelial cell shape, whereas $CD90^+$ cells showed a mesenchymal VEC shape (Fig. 5C and Supporting Fig. 3C). FACS analysis indicated that P12 HCC cells showed abundant expression of vascular endothelial growth factor receptor (VEGFR) 1 and a vascular endothelial marker endoglin (CD105) (Fig. 5D). By contrast, P4 and P7 HCC cells did not express these vascular endothelial markers (data not shown). Lung metastasis was detected in NOD/SCID mice transplanted with P12 HCC cells, but not in mice transplanted with P4 and P7 HCC cells (Fig. 5E,F).

Taken together, these results suggest that the tumorigenic and metastatic capability of primary HCC may depend on the presence of distinct $EpCAM^+$ or $CD90^+$ CSCs. $EpCAM^+$ cells were associated with a high tumorigenic capacity with hepatic epithelial stem cell features, whereas $CD90^+$ cells were related to the metastatic propensity with VEC features.

Suppression of Lung Metastasis Mediated by $CD90^+$ CSCs by Imatinib Mesylate. We previously demonstrated that Wnt/β-catenin signaling inhibitors could successfully attenuate the tumorigenic capacity of $EpCAM^+$ CSCs in HCC.[8,10] To explore the potential molecular targets activated in $CD90^+$ CSCs, we investigated the expression of the known VEC markers, CD105, VEGFR1 (encoded by *FLT1*), and

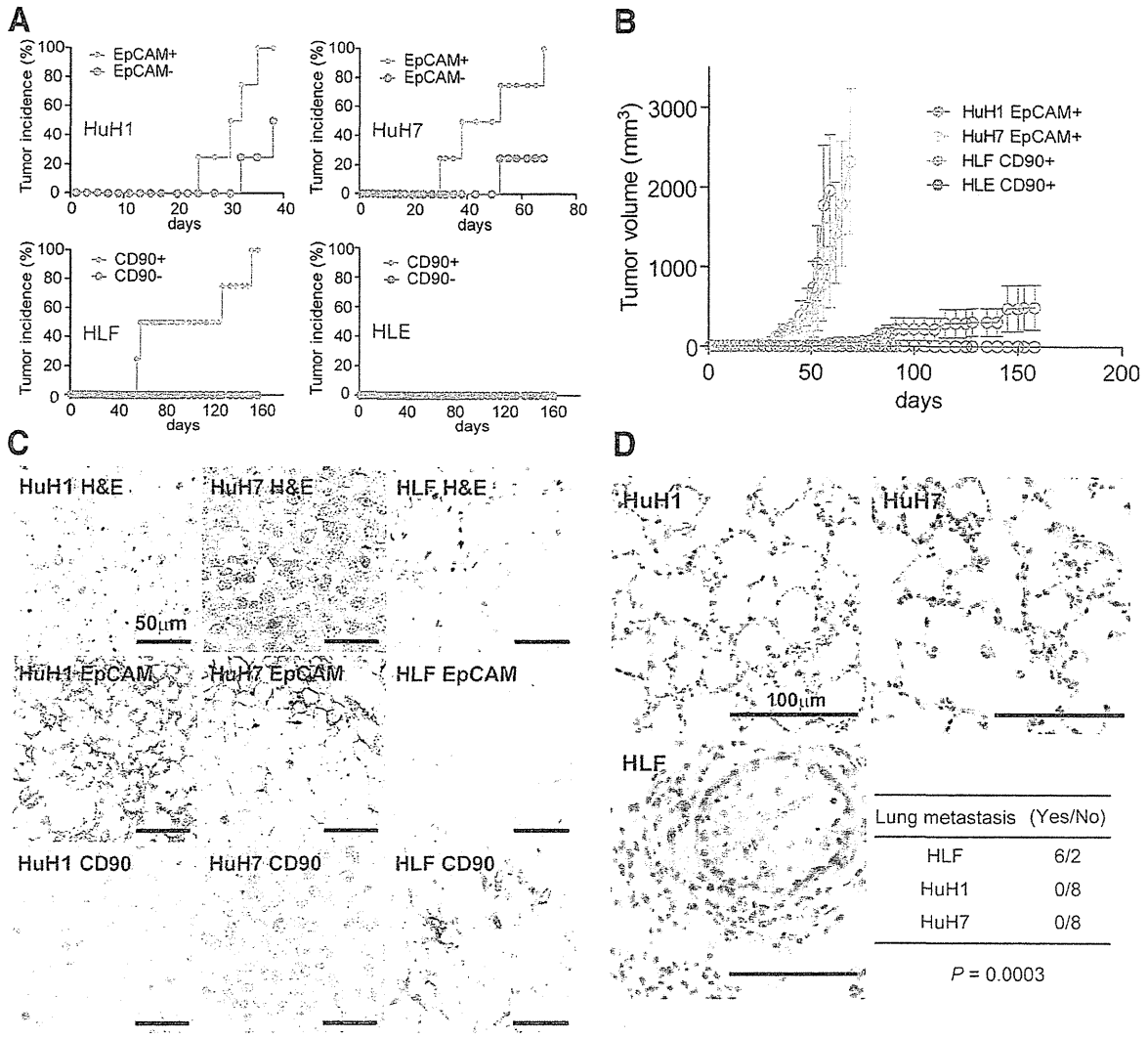

Fig. 4. Distinct tumorigenic/metastatic capacities of HCC cell lines defined by EpCAM and CD90. (A) Tumorigenicity of 1×10^5 cells sorted by anti-EpCAM (HuH1 and HuH7) or anti-CD90 (HLE and HLF) Abs. Data are generated from 8 mice/cell line. (B) Tumorigenic ability of $EpCAM^+$ and $CD90^+$ sorted cells in NOD/SCID mice. Aggressive tumor growth in the SC lesion was observed in $EpCAM^+$ HuH1 or HuH7 cells, compared with $CD90^+$ HLE or HLF cells. $EpCAM^+$ (1×10^5) or $CD90^+$ cells were injected. Tumor-volume curves are depicted as mean ± standard deviation of 4 mice/group. (C) Histological analysis of $EpCAM^+$ or $CD90^+$ cell-derived xenografts. Hematoxylin and eosin (H&E) staining of a SC tumor (upper panels) and IHC of the tumor with anti-EpCAM (middle panels) or anti-CD90 Abs (bottom panels) are shown (scale bar, 50 μm). (D) Metastasis was evaluated macroscopically and microscopically in the left and right lobes of the lung separately in each mouse (n = 4) (scale bar, 100 μm).

c-Kit (encoded by *KIT*), in cell lines and showed that they were abundantly expressed in $CD90^+$ cell lines, but not $EpCAM^+$ cell lines (Fig. 6A). No expression of VEGFR2 was detected in this set of cell lines, suggesting that molecular reagents specifically targeting VEGFR2 may have no effects on $CD90^+$ CSCs. CD44, a stem cell marker that functionally regulates redox status and is a potential target of $CD90^+$ CSCs, was also abundantly expressed in $CD90^+$ cell lines (Supporting Fig. 4A), consistent with previous data.[5,13] No significant difference was detected in the expression of the hematopoietic marker, CD34, or ABCG2 between $EpCAM^+$ and $CD90^+$ cell lines (Supporting Fig. 4A).

Among these molecular targets, we focused on the characterization of c-Kit because the c-Kit tyrosine kinase inhibitor, imatinib mesylate, is readily available, is widely used for the treatment of gastrointestinal stromal tumor with activation of c-Kit, and may have potential antitumor activity against a subset of HCC.[14] We explored the effect of imatinib mesylate on HCC cell lines and found that treatment with 10